JOURNAL OF SPACECRAFT AND ROCKETS
Vol. 40, No. 5, September–October 2003
This paper reprinted from IAS–RAeS Proceedings—1955, pp. 241–276

Hypersonic Flow

LESTER LEES†

SUMMARY

This paper discusses some of the areas in which our understanding of hypersonic flows has progressed in recent years—with special reference to the hypersonic similarity concept and the hypersonic approximations; the interaction between the boundary layer over a slender body and the external inviscid flow; and the flow over blunt bodies, including the heat-transfer problem.

When the inviscid pressure distributions predicted by the hypersonic approximations (Newtonian, shock-expansion, tangent-wedge, and cone) are compared with "exact" solutions and experimental data, it becomes evident that this problem is effectively solved for sharp-nosed slender wings and bodies of revolution. The shock-expansion and tangent-wedge (or tangent-cone) method may also be used to construct the flow field. An examination of the equations of motion shows that the simple tangent-wedge (or cone) method, which is thought by some to be largely semiempirical, actually has a sound theoretical basis.

At hypersonic speeds the flow over sharp-nosed slender shapes cannot be properly treated without considering boundary-layer–external flow interactions. Since the mass flux through the boundary layer is small, the streamlines entering the boundary layer are very nearly parallel to the outer edge. In other words, the flow inclination there is the sum of the body inclination and the slope of the boundary layer, and the local pressure is related to the boundary-layer growth rate by means of the tangent-wedge (or tangent-cone) approximation. A second relation between these quantities is provided by the Prandtl boundary-layer equations. For both strong and weak interactions over inclined wedges, for example, the governing viscous interaction parameter is (Mach Number)^3/(Reynolds Number)$^{1/2}$.

The straightforward approach to this problem seems to be adequate when the Reynolds Number based on leading-edge thickness, Re_t, is a few hundred or less. For larger Re_t the experimentally measured induced pressures on flat surfaces suggest that the strong bow shock decays surprisingly slowly at high Mach Numbers and that the expansion waves reflected from this shock and impinging on the surface may overwhelm the purely viscous effect.

For blunt bodies the modified Newtonian approximation in the form $C_p/C_{pmax} = \sin^2 \theta_b$ is highly accurate for Mach Numbers above 2.0, even for shapes with rapidly varying (convex) curvature. Current treatments of heat transfer over such bodies are limited to small temperature differences between gas and body surface. For this case the agreement between Sibulkin's theoretical result and experiments in the Mach Number range $2 < M < 5$ is good. For large temperature differences an expression quite similar to Sibulkin's is derived based on gas properties evaluated at the surface temperature. This problem appears to be a fruitful one for the investigation of the influence of high temperature gas phenomena on hypersonic fluid mechanics.

SYMBOLS

a	=	sound speed
c	=	airfoil chord
C	=	Chapman-Rubesin factor in relation $(\mu/\mu_\infty) = C(T/T_\infty)$
C_p, C_v	=	specific heats at constant pressure and constant volume, respectively
C_f	=	local skin-friction coefficient

† Associate Professor of Aeronautics and Applied Mechanics, California Institute of Technology, Pasadena, Calif. Now, Professor of Aeronautics, C.I.T.

The author would like to express his appreciation to Dr. Clark B. Millikan for reading the manuscript and to Dr. Henry T. Nagamatsu and the GALCIT hypersonic research group for their kind assistance in preparing this paper.

C_H = local heat-transfer coefficient, or Stanton Number, defined by $q = C_H \rho_\delta u_\delta (h_{s_\delta} - h\omega)$

C_p = pressure coefficient, $\{(p - p_\infty)/[(1/2)\rho_\infty U_\infty{}^2]\}$

D = nose diameter

g = acceleration of gravity, 32.2 ft/sec.^{2}

h = film coefficient, $q/(T_{s_\delta} - T\omega)$; also static enthalpy

h_s = stagnation enthalpy

H = h_s/h_{s_δ}

k = thermal conductivity

l = body length

M = Mach Number, u/a

$\mathfrak{M}$ = molecular weight

Nu = Nusselt Number, hD/k

p = static pressure

Pr = Prandtl Number, $[(C_p\mu)/k]$

q = local heat-transfer rate, per unit area, per unit time

r = radius from origin of polar coordinates

r_0 = radius of cross section of body of revolution

Re = Reynolds Number

Re_x = $[(\rho_\infty u_\infty x)/u_\infty]$

Re_{xb} = $[(\rho_b u_b x)/\mu_b]$

Re_D = $[(\rho_2 u_2 D)/\mu_2]$

R_0 = universal gas constant

s = distance along body surface from stagnation point or from leading-edge or nose vertex

t = time, also leading-edge thickness and airfoil thickness

T = absolute gas temperature

u, v, w = velocity components parallel to x, y, z axes, respectively

u_r, u_θ = radial and circumferential velocity components

$U_\infty, \dot{U}_\infty$ = flight velocity and acceleration in flight direction, respectively

w = u/u_∞ or u/u_1 in boundary-layer discussion

x, y, z = x-axis in relative wind direction, y-axis along right wing, and z-axis vertical, with origin at leading-edge or nose vertex

α = angle of pitch or yaw

β = pressure gradient parameter

γ = ratio of specific heats, C_p/C_v

δ = boundary-layer thickness

δ^* = boundary-layer displacement thickness, $\displaystyle\int_0^\infty \left(1 - \frac{\rho}{\rho_\infty}\frac{u}{u_\infty}\right) dz$

η = nondimensional distance normal to surface in equivalent low-speed boundary-layer flow, $\left[y \cdot \sqrt{u_\infty/(\nu_\infty x C)}\right]_i$

ϑ = flow inclination, also ray angle

θ_s = shock angle

κ = surface curvature, $d\theta_b/ds$

λ = $\dfrac{[(1/p_\infty)(dp/ds)]_{\text{exact}}}{[(1/p_\infty)(dp/ds)]_{\text{approx.}}}$

μ = absolute viscosity

ν = kinematic viscosity, μ/ρ

ρ = gas density

σ = angle between normal to a surface element and flight direction

τ = transit time for airfoil, c/U_∞

ϕ = ray angle in plane transverse to body axis

$\bar{\chi}$ = viscous interaction parameter, $(M^3/\sqrt{Re})\sqrt{C}$

Subscripts

b, c, w = inviscid flow quantities at the surface of an arbitrary body, a cone, and a wedge, respectively
s = stagnation conditions
w = gas properties evaluated at actual surface temperatures
TC = tangent-cone
TW = tangent-wedge
SE = shock-expansion
N. + C.F. = Newtonian plus centrifugal force
0 = zeroth order approximation
2 = conditions just behind a shock wave
∞ = ambient flight or free-stream conditions
δ = quantities at outer edge of boundary layer

(1) Introduction and General Survey

Because of the rapid development of rocket propulsion technology, ultra-high-speed flight is now much closer to reality than anyone would have predicted 10 years ago. But successful solutions of some of the major problems in this flight regime, and particularly of the heat-transfer problem, depend to a great extent upon a scientific knowledge of hypersonic fluid mechanics. It is the purpose of this paper to discuss some of the areas in which our understanding of hypersonic flows has progressed in recent years and to indicate the directions of current research in this field.

First of all, in what respects does hypersonic flow† differ significantly from the more familiar supersonic flow? The most important differences are: (a) the closeness of shock waves and body surface and the existence of hypersonic similarity; (b) the interaction between the boundary layer over a slender body and the "external" inviscid flow; (c) the appearance of high temperature gas phenomena. Suppose that we consider the broad features of each of these hypersonic effects before entering upon a more detailed discussion.

At very high Mach Numbers Tsien[1] showed that potential flow over geometrically similar airfoils and bodies of revolution is dynamically similar when the product of Mach Number and thickness ratio, $K = M_\infty t/c$, is a constant.‡ In other words, the flow is characterized solely by the ratio of maximum velocity normal to the surface to ambient sound speed. Later Hayes[2] extended this concept of hypersonic similarity to include general steady and unsteady flows with vorticity. The physical basis for hypersonic similarity lies in the fact that at high flight Mach Numbers, the local Mach Numbers over slender bodies at low angles of attack are also high, and the shock waves and Mach waves are practically parallel to the flight direction (Fig. 1). The flows in any two fixed planes normal to the flight direction are practically independent of one another because the time required for a sound-wave signal to

† The term "hypersonic" was introduced by Tsien[1] and quickly superseded the older term "ultrasupersonic," which had the tendency to become confused with ultrasonic, or high-frequency, sound waves.

‡ Here dynamic similarity is expressed in terms of pressure ratio p/p_∞, density ratio ρ/ρ_∞, etc. Of course γ must also be constant. For bodies of revolution $K = M_\infty/(l/d)$, where l/d is fineness ratio.

traverse the distance between these planes is much longer than the transit time of the body between these planes. Thus the flow in any fixed transverse plane depends only on the history of the local body inclination with time.

A fixed observer watching the passage of a slender hypersonic airfoil across a narrow slit normal to the flight direction sees a vertical gas motion quite similar to that produced by a moving piston in a long, straight tube (Fig. 1). Suppose that the airfoil shape is given by $z = z_{max}f(x/c)$. Then the equivalent piston motion in the transverse direction is given by $z = z_{max}f(t/\tau)$, where t is measured from the instant the leading edge crosses the slit, and τ is the duration of piston motion $= c/U_\infty$. In the piston problem it is well known that for any given funtion $f(t/\tau)$ the gas motion depends only on

$$(w_{max}/a_\infty) = (1/a_\infty)(dz/dt)_{max} \sim (z_{max}/a_\infty\tau) = (z_{max}/U_\infty\tau)M_\infty = M_\infty t/c$$

for the hypersonic airfoil. Therefore geometrically similar slender airfoils produce the same gas motion at hypersonic speeds if the thickness ratio is inversely propor-

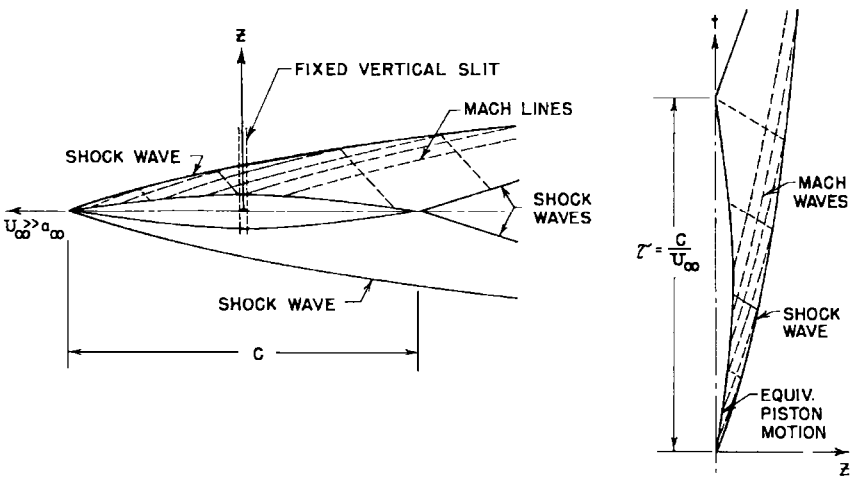

FIG. 1. Equivalence of steady hypersonic motion of plane ogive and nonsteady piston problem.

tional to the flight Mach Number. The same reasoning is readily extended to slender bodies of revolution, planar bodies, and wing-body combinations at small angles of incidence, and also to body oscillations, including aeroelastic motions.† Hypersonic similarity has been applied to most of these cases in an extensive series of papers.[3–8]

It is now generally agreed that hypersonic similarity is applicable not only for $M_\infty \gg 1$, as postulated in the original derivation, but when $M_\infty^2 - 1 \cong M_\infty^2$, or $M_\infty > 2.5 - 3.0$, *and* $\theta_b < 20°$, where θ_b is the inclination of a surface element to the flight direction. When these conditions are satisfied, the similarity parameter may take any value from zero to ∞, and the fact that the shock waves and Mach waves

† At hypersonic flight speeds, the effect of accelerations of the body along and normal to the flight path is generally negligible. The important parameter here is the magnitude of the change in flight velocity or relative wind direction during the time interval required for a fluid particle to flow over the body, compared to the flight velocity, or $(\dot{U}_\infty L/U_\infty)/U_\infty = \dot{U}_\infty L/U_\infty^2$. For a body 100 ft. in length at a flight speed of 10,000 ft. per sec., this ratio is only 0.01 even if $\dot{U}_\infty = 300g$.

propagate away from the body in a direction not quite normal to the flight direction introduces errors of order $1/M_\infty^2$ or θ_b^2, whichever is larger.

Unless $K \ll 1$, hypersonic flow problems are essentially nonlinear, and approximate methods for constructing the flow are extremely desirable. Several of these hypersonic approximations are based on the fact that shock waves approach the body surface very closely as $K \to \infty$. In fact Newton's particle concept, which is now enjoying a renascence in the hypersonic flow regime, implies that the shock wave coincides with the body surface. The significance of this concept in modern aerodynamics was clarified by von Kármán[9] and Busemann.[10] According to Newton the fluid particles ahead of a body in flight are not disturbed by the body until they strike the surface, whereupon they lose all of their relative momentum normal to the surface and then flow tangentially to the surface with no further change in velocity. The impact pressure is given by $p - p_\infty = \rho_\infty U_\infty^2 \cos^2 \sigma$, where σ is the angle between the normal to the surface element and the flight direction. In Newton's "model" the mass flow between any two streamlines ahead of the shock would have to be squeezed into a narrow zone between the shock and the body surface, and the density ratio across the shock wave would have to be very high. If one thinks of a polyatomic gas molecule with a very large number of internal degrees of freedom and a high specific heat capacity, the temperature rise across a shock wave in such a gas is small. Since the pressure ratio is large at high speeds so is the density ratio, and Newton's statement must be nearly correct. But what is the situation for a diatomic gas or a diatomic gas mixture, such as air?

According to the oblique shock relations, the density ratio ρ_2/ρ_∞ across the shock wave approaches $(1 + n)$ when $M_\infty \sin \theta_s \to \infty$, where "$n$" is the number of internal degrees of freedom of the gas molecule, and θ_s is shock angle. For a blunt body, the ratio of the detachment distance between bow shock and body surface to the radius of curvature of the shock is of the order of ρ_∞/ρ_2 at very high Mach Numbers; while for slender airfoils, the difference between shock angle θ_s and flow angle θ behind the shock is equal to $\theta/(\rho_2/\rho_\infty - 1) = \theta/n$. In air at ordinary temperatures, $n = 5$, and the limiting values, as $M_\infty \to \infty$, are $\rho_2/\rho_\infty = 6$ and $\theta_s - \theta = 0.20\,\theta$. At somewhat higher temperatures, when the vibrational modes of nitrogen and oxygen are excited, $n = 7$, $\rho_2/\rho_\infty = 8$, and $\theta_s - \theta = 0.14\,\theta$. At still higher temperatures, dissociation and ionization act as "heat sinks" and reduce the temperature ratio even further, so that $\rho_2/\rho_\infty \to 10 - 11$ and $\theta_s - \theta \to 0.10\,\theta$. For slender bodies of revolution, the shock wave is even closer to the body surface [Section (2)]. Clearly, the Newtonian concept is a useful approximation when $M_\infty \sin \theta_b$ is "sufficiently large."

For slender sharp-nosed bodies, the Newtonian approximation is improved by the addition of the centrifugal force correction, as shown by Busemann,[10] by Grimminger, Williams, and Young,[11] and by Ivey, Klunker, and Bowen.[12] As we shall see later, [Section (4)], for a blunt-nosed body of revolution with convex curvature, the ratio of local over-pressure to the maximum over-pressure at the forward stagnation point follows the simple Newtonian $\sin^2 \theta_b$ law very closely for $M_\infty > 2.0$.

A parallel approach to the Newtonian concept of a purely local dependence of surface pressure on body inclination is contained in the "tangent-wedge" approximation for slender airfoils at hypersonic speeds. In this method, the pressure at any

point on the surface, where $\theta = \theta_b$, is regarded as identical with the pressure on a semi-infinite wedge of half-angle θ_b at the same flight (not local) Mach Number. The analog for slender bodies of revolution is the "tangent-cone" approximation. These methods attempt to account for the fact that the shock wave is close to the surface but not coincident with it. When the theoretical basis for these approximations is examined [Section (2)], it will be found that their high degree of accuracy over most of the range in which hypersonic similarity is applicable is by no means coincidental.

Another hypersonic approximation for slender bodies is the "shock-expansion" method, which was introduced originally by Epstein[13] and has since been developed in quite general form by Eggers, Syvertson, and Savin[14–18] for both steady and nonsteady flows. This approximation is based mainly on their discovery that—at least for γ near 1.40—the expansion waves from the surface of a body are almost completely absorbed in the nose shock wave, except near shock detachment. All of these approximations are compared with "exact" solutions in Section (2).

Because the shock wave is so close to the body at hypersonic speeds, the boundary layer over the surface of a slender body must exert a strong influence on the flow field. The importance of this boundary-layer shock wave interaction was first recognized by Tsien, who encouraged S. F. Shen[19] to investigate the problem under his direction. At low speeds and high Reynolds Numbers, Prandtl's concept of a thin boundary layer states that the flow over a body is first computed as if the fluid were inviscid, and the development of the boundary layer is then obtained on the basis of this "external" inviscid flow. All of the fluid entering the boundary layer usually has the same total head and total enthalpy, and pressure and velocity along the "outer" edge of this layer are connected by Bernoulli's relation. Since the local streamline deflection induced by the boundary layer is of order $1/\sqrt{Re_x}$, the boundary-layer effect on the flow field over a slender airfoil is of order $1/Re_x$ at low speeds and is usually negligibly small, except at high angles of attack.

At supersonic, and especially hypersonic, speeds the situation is quite different [Section (3)]. The deceleration of the gas as it penetrates the viscous layer generates high temperatures in this region. As a result, the hypersonic laminar boundary layer is from 10 to 100 times thicker than it is at low speeds at the same Reynolds Number (Re_x), and the outward streamline deflection induced by this thick boundary layer amounts to a significant change in the "effective shape" of the body. At high flight speeds even small changes in flow inclination at the body surface produce large pressure changes, and the pressure gradients induced by the boundary-layer curvature in turn "feed back" into the viscous layer and effect its rate of growth. In addition, the change in effective shape of the body surface alters the shape of the leading-edge or nose shock wave, and the resultant entropy changes are transported downstream along the streamlines. At hypersonic speeds, the mass flux in the boundary layer is very small, so that the streamlines that enter the boundary layer have previously crossed the shock wave far upstream near the leading-edge where the shock wave is strong and highly curved. In other words, the whole development of the boundary layer and the induced pressure field may depend to some extent upon conditions around the nose or leading-edge region.

For blunt bodies (or the compression side of slender bodies at high angles of

attack) the flow behind the nose or leading-edge shock wave is subsonic or low supersonic even at very high flight speeds, and the interaction between the boundary layer and the external flow is generally negligible at high Reynolds Numbers. For this reason, it seems logical to treat the hypersonic flow over slender and blunt bodies separately in the subsequent discussion. A more difficult problem, which is of considerable technical interest, is the case of the slender body with a rounded nose or leading edge to reduce the heat-transfer rate. Here the hypersonic approximations and the Prandtl boundary-layer theory must both be carefully reexamined because of the strong vorticity introduced into the flow by the detached shock wave at the nose.

High temperature gas phenomena in high-speed flight have already been brought into the discussion of the proximity of shock wave and body surface. At hypersonic speeds, the detached shock wave in front of a blunt nose converts practically all of the kinetic energy associated with the flight velocity into enthalpy, or thermal energy. At the "escape velocity" of 26,400 ft. per sec., for example, this energy amounts to 14,000 B.t.u. per lb. of air, which is sufficient to dissociate the nitrogen and oxygen molecules almost completely, to produce a small but important ion concentration, and to still raise the gas temprature to about 16,000°R. So long as the gas is in a state of thermodynamic equilibrium at all times, the problem is no different in principle from the low temperature case, but the calculations may be much more tedious. For example, the equation of state modified to include the free electrons is $p = \rho(R_0/\mathfrak{M})T\ (1 + \alpha)$, where α is the fraction of gas ionized, and $\mathfrak{M}$, the molecular weight, is a function of the equilibrium concentrations of the components which depend on pressure and temperature (enthalpy). Calculations of the state of the gas behind a normal shock wave have been carried out by Döring, and Burkhardt,[20]† Bethe, and Teller,[21]† Kantrowitz, Resler, and Lin,[22] and others. In all of these calculations the pressure is not much affected, since $p_2 - p_\infty = \rho_\infty U_\infty{}^2\ [1 - (\rho_\infty/\rho_2)]$ and ρ_∞/ρ_2 is small for strong shocks; however, the temperature, density, and specific heats differ greatly from the values based on low temperature gas properties.

For a slender body, the gas temperatures in the inviscid flow field outside the boundary layer are much lower than the temperatures behind a normal shock, and high temperature effects are much less spectacular. Ivey and Cline[23] have computed the effect of variable specific heats on the flow across an oblique shock wave, and Kraus[24] examined this effect for the shock-expansion method. In Fig. 2, the similarity concept is applied to the calculations of Ivey and Cline, which were carried out for sea-level initial conditions.‡ Along the lower dashed curve of flow deflection vs. flight Mach Number, $K = M_\infty\theta_w = 1.75$. This curve is the locus of all pairs of $M_\infty - \theta_w$ values for which the density ratio across the shock is only 1 per cent larger than the density ratio for $\gamma = 1.40$ and the shock angle is decreased by

† These calculations utilize the older and lower value for the dissociation energy of nitrogen and ignore the thermal ionization of NO. These "errors" were corrected recently by Kantrowitz and coworkers.

‡ It should be remarked that in order for hypersonic similarity to be strictly applicable, not only must $K = M_\infty t/c$ be constant, but the ambient temperature must be the same, and also the ambient pressure if appreciable dissociation occurs.

0.4 per cent, while the pressure ratio is hardly affected. Along the upper full curve, $K = 3.50$, and the effects are noticeable but still small.

Probably the most serious gap in our knowledge of high temperature phenomena is the lack of information about nonequilibrium processes in air. It is possible that a solid surface is the only effective catalyst or energy sink for recombination of atoms or de-excitation of ions. In that case, the fluid mechanics in the boundary layer of a blunt-nosed body may be quite different from the conventional analysis based on molecular heat conduction. Since these important questions are at present the subject of intensive research, no further account will be taken of them in this paper. In fact, in most of our subsequent discussion, the gas is to be treated as an ideal gas in thermodynamic equilibrium, with certain average specific heats. This procedure is adopted in order to bring out some of the fluid-mechanical aspects of hypersonic flow as simply as possible.

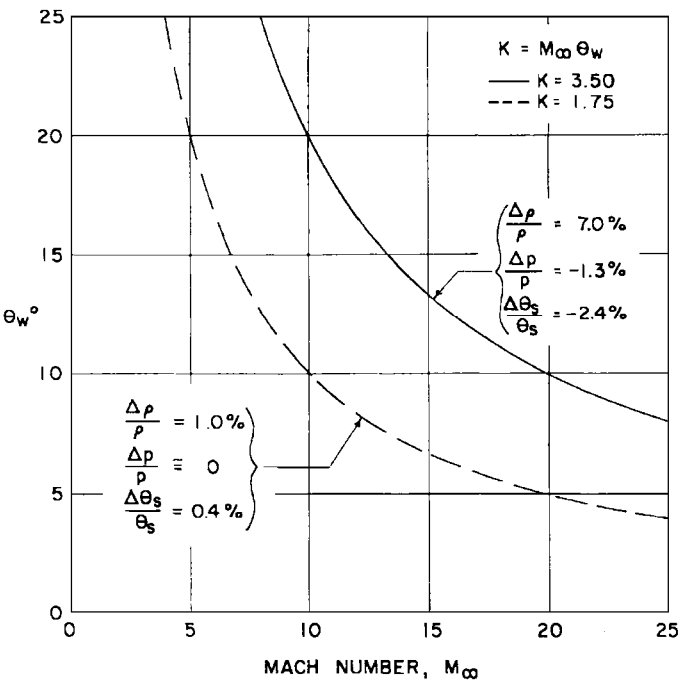

FIG. 2. Effect of temperature-dependent specific heats on flow across an oblique shock wave.

(2) HYPERSONIC APPROXIMATIONS FOR PLANAR BODIES AND SLENDER BODIES OF REVOLUTION

(2.1) Tangent-Wedge and Tangent-Cone Approximations

The simple relation between pressure and local streamline inclination, contained in the tangent-wedge approximation (hereafter called *TW*), is derived from the oblique shock-wave equation by imposing the conditions for hypersonic similarity—i.e., $M_\infty^2 - 1 \cong M_\infty^2$, or $M_\infty > 2.5 - 3.0$, and $\tan\theta = \sin\theta = \theta$ ($\theta < 20°$, approximately). According to the oblique shock relations

$$\rho_2/\rho_\infty = \tan\theta_s/\tan(\theta_s - \theta_w) = (\gamma + 1)/\{\gamma - 1 + [2/(M_\infty^2 \sin^2\theta_s)]\} \quad (1)$$

$$(p_2/p_\infty) = 1 + [2\gamma/(\gamma + 1)](M_\infty^2 \sin^2\theta_s - 1) \quad (2)$$

By solving Eq. (1) for θ_s with the restrictions mentioned above, one obtains

$$M_\infty\theta_s = [(\gamma + 1)/4]M_\infty\theta_w + \sqrt{1 + \{[(\gamma + 1)/4]M_\infty\theta_w\}^2} \tag{3}$$

and substituting Eq. (3) into Eq. (2), one finds that

$$p_2/p_\infty = 1 + [\gamma(\gamma + 1)/4]K_w^2 + \gamma K_w\sqrt{1 + [(\gamma + 1)/4]^2K_w^2} \tag{4a}$$

or $$C_p = (2/\gamma M_\infty^2)[(p/p_\infty) - 1] = \theta_w^2\{[(\gamma + 1)/2] + \sqrt{[(\gamma + 1)/2]^2 + (4/K_w^2)}\} \tag{4b}$$

where $$K_w = M_\infty\theta_w$$

When the airfoil shape is expressed as $z = z_{max}f(x/c)$, the local value of K is $M_\infty t/c \times \{[f'(x/c)] \pm [\alpha/(t/c)]\}$, where the plus sign applies to the lower surface and the minus sign to the upper surface. In the limiting case $K_w \ll 1$, TW reduces to the series

$$p/p_\infty = 1 + \gamma K_w + \{[\gamma(\gamma + 1)]/4\}K_w^2 + \{[\gamma(\gamma + 1)^2]/32\}K_w^3 + \ldots$$

which is the well-known Busemann expansion (for $M_\infty^2 - 1 \cong M_\infty^2$) up to terms of order K_w^2; the Busemann series itself is identical with the shock-expansion method up to terms of order K_w^3.†

Linnell[26] was the first to put the oblique shock relations in the simple form of Eqs. (3) and (4), but he utilized them only for the leading-edge shock wave and employed the shock-expansion method over the rest of the airfoil surface. Ivey and Cline[23] derived these relations apparently independently and compared the approximate values of pressure ratio with those predicted by the full equations; the agreement between the two in the hypersonic range is phenomenal, as shown also by von Kármán.[27] They applied TW to the calculation of pressure distributions and lift and drag coefficients for a symmetrical double-wedge airfoil, with excellent results.‡ These investigators also noticed that when K_w is replaced by $\theta_w\sqrt{(M_w^2 - 1)}$ in Eq. (4b), the approximation is extended over the whole supersonic range with good accuracy. Recently Van Dyke[8, 28, 29] showed that this result is general; when K is replaced by $\sqrt{M^2 - 1}\,\theta$ in the hypersonic thin-body theory, the error is of order θ^2, while the error in the linearized supersonic theory for flat wings is of order θ^2 or $[\theta/(\sqrt{M_\infty^2 - 1})]$—whichever is larger—and the error in the linearized theory for slender bodies of revolution is of order θ^2 or $[\theta^2/(M_\infty^2 - 1)]$—whichever is larger.

Since the pressure given by TW is very nearly correct at the leading edge, a more instructive measure of the accuracy of this approximation is the initial pressure gradient on a plane ogive. According to TW

$$\frac{1}{\kappa}\left(\frac{1}{p_\infty}\frac{dp}{ds}\right) = \gamma M_\infty\left\{\frac{\gamma + 1}{2}K_w + \frac{1 + 2[(\gamma + 1)/4]^2K_w^2}{\sqrt{1 + [(\gamma + 1)/4]^2K_w^2}}\right\} \tag{5}$$

† The coefficient of K_w^3 in the Busemann series,[25] corresponding to the term $(C_3 - D)\theta_w^3$, is $3/32\gamma(\gamma + 1)^2$ for $M_\infty^2 - 1 \cong M_\infty^2$. The series given here is convergent for $K_w \leqq 4/(\gamma + 1)$.

‡ It is remarkable that at least for $\gamma = 1.40$, Ivey and Cline find that Eq. (4) also gives good agreement with the Prandtl-Meyer expansion starting from the free-stream Mach Number, where $K_w < 0$.

where s is distance along the body surface and $\kappa = (d\theta_w/ds)$ is the curvature. Kraus[24] has tabulated the exact value of $(1/\kappa)[(1/p_\infty)(dp/ds)]$, calculated by the method of characteristics for $\gamma = 1.40$. In Fig. 3a, the ratio

$$\lambda_{TW} = \frac{[(1/p_\infty)(dp/ds)]_{\text{exact}}}{[(1/p_\infty)(dp/ds)]_{TW}}$$

is plotted as a function of K for this value of γ.

The limiting value of $(1/\kappa)[(1/p_\infty)(dp/ds)]_{\text{exact}}$ as $K_w \to \infty$ is $\{[3\gamma^2(\gamma+1)] \div [2(2\gamma-1)]\} M_\infty{}^2\theta_w$. According to TW,

$$(1/\kappa)[(1/p_\infty)(dp/ds)]_{TW} \to \gamma(\gamma+1)M_\infty{}^2\theta_w \qquad \text{as } K_w \to \infty$$

so that

$$\lambda_{TW} \to [3\gamma/(2\gamma-1)]$$

This limiting value of λ_{TW} is plotted as a function of γ in Fig. 3b.

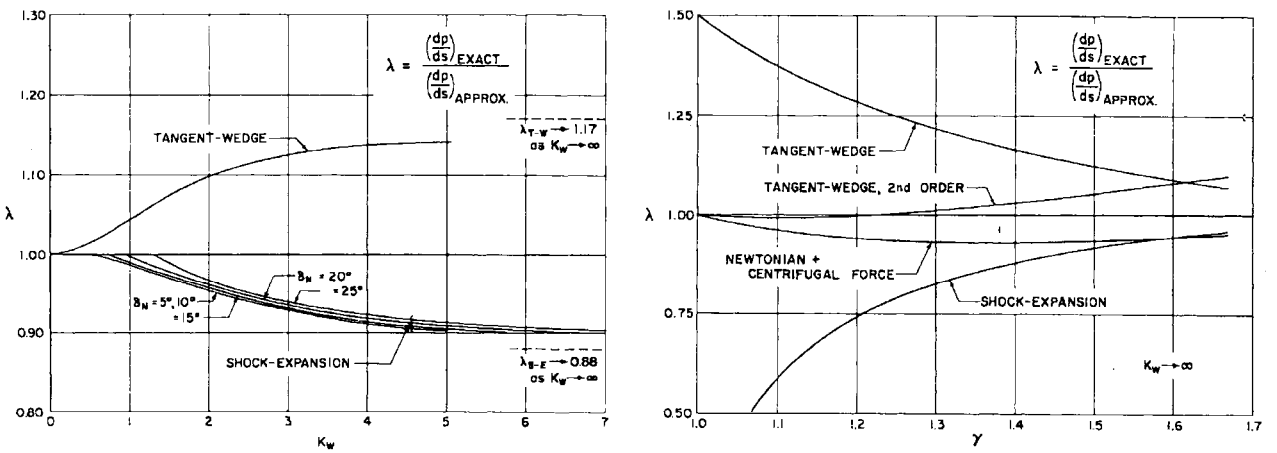

FIG. 3a (*left*). Initial pressure gradient ratio on plane ogive-hypersonic approximations. $\gamma = 1.40$. FIG. 3b (*right*). Limiting values of initial pressure gradient ratio on plane ogive.

The approximations inherent in TW and the underlying reasons for its high degree of accuracy for $\gamma \cong 1.4$ are brought out most clearly by considering the limiting case $K_w \to \infty$. For a sharp-nosed slender airfoil in this case, $[(dz_s/dx) \div (dz_b/dx)] \cong z_s/z_b$, according to this approximation (Fig. 4). In other words, the tangents to the shock wave and the body surface intersect in a point on the flight axis,† and the approximation states that pressure and flow inclination are *constant* along the normal to the body surface, which is very nearly the vertical line between shock wave and body surface.

Now this statement is in error for at least two reasons, but these two effects tend to cancel each other: (a) On a convex body, for example, the pressure on the body surface is actually *lower* than the pressure just behind the shock wave at the same x-station because of centrifugal force, so that TW *overestimates* the surface pressure on this account; (b) on a convex body, the density is falling along the body surface and, by continuity, the velocity component normal to the flight axis must *increase* toward the shock wave. Therefore, the flow inclination just behind the shock is *larger* than the body inclination, the pressure just behind the shock is

† Of course this point is different for every choice of x.

higher than predicted by TW, and, therefore, so is the surface pressure. A quantitative estimate of these compensating errors is worked out in the Appendix. The result is as follows:

$$p_b/p_\infty = (\gamma/2)(\gamma + 1)M_\infty{}^2\theta_b{}^2 + M_\infty{}^2 z_{b\kappa}[\gamma - (\gamma^2 - 1)]$$

where the γ in the brackets represents the centrifugal force effect and the $(\gamma^2 - 1)$ represents the effect of the increase in flow inclination from body surface to shock. In the limiting case $\gamma \to 1$, this corrected form of TW is exact and is, of course, identical with the Newtonian approximation including centrifugal force.

For this "corrected," or second-order TW,

$$(1/\kappa)(1/p_\infty)(dp/ds) \to (2\gamma + 1)M_\infty{}^2\theta_w \qquad \text{as } K_w \to \infty$$

so that

$$\lambda_{TW_{\text{2nd order}}} \to [3\gamma^2(\gamma + 1)]/[2(4\gamma^2 - 1)]$$

This limiting value of λ is shown in Fig. 3b. Clearly, the corrections to TW discussed here represent nearly all of the error involved in this approximation and help to explain the success of this simple method.

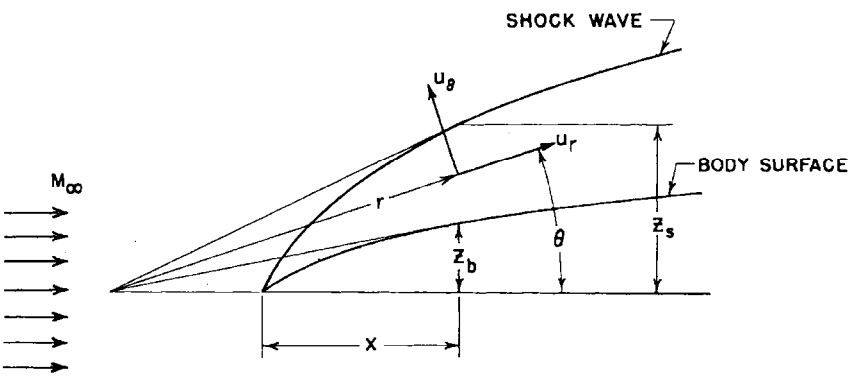

FIG. 4. Tangent-wedge approximation for $M_\infty \to \infty$.

A parallel discussion can be given for the tangent-cone (TC) approximation, but the details will not be reproduced here. According to this approximation, the pressure at any point on the surface of a slender body of revolution at arbitrary angles of pitch and yaw is identical with the Taylor-Maccoll value on a semi-infinite unyawed circular cone of half-angle equal to the local inclination of the streamline with respect to the flight direction. The free-stream Mach Number for the equivalent cone is the body flight Mach Number. Halbmillion and Kulishek[30] (and others) noticed that TC gives good results for slender unyawed ogives of revolution.

By utilizing the concept of hypersonic similarity, the present author[31] obtained simple algebraic expressions for the pressure on the surface of an unyawed cone in the range $1 < K_c < \infty$, which put TC on the same footing as TW. These relations were obtained by substituting the Taylor's series expansions for the analytical solutions of the conical flow equations into the boundary conditions at the shock surface and then imposing the conditions for hypersonic similarity *and* the limitation that $[(\theta_s - \theta_c)/\theta_c]$ is "small"—i.e., the shock cone is close to the body. With these approximations,

$$K_s = [(\gamma + 1)/(\gamma + 3)]K_c + \sqrt{[(\gamma + 1)/(\gamma + 3)]^2(K_c)^2 + [2/(\gamma + 3)]} \quad (6)$$

$$C_{D_c}M_\infty^2 = C_{p_c}M_\infty^2 = (2/\gamma)[(p_c/p_\infty) - 1]$$

where

$$p_c/p_\infty = 1 + [2\gamma/(\gamma + 1)](K_s^2 - 1) + \gamma(K_s - K_c)^2\{(\gamma + 1)/[\gamma - 1 + (2/K_s^2)]\} \quad (7)$$

These approximate relations are compared with the Kopal[32] values for cones of 5°, 10°, 15°, and 20° half-angle in Fig. 5. For $K_c > 1$, the difference between exact and approximate values is less than 7 per cent. For $K_c < 1$, the von Kármán slender body approximation to linearized supersonic theory is useful; here

$$C_pM_\infty^2 = 2K_c^2 \log_e (2/K_c)$$

As an index of the accuracy of the tangent-cone approximation the ratio

$$\lambda_{TC} = \frac{[(1/p_\infty)(dp/ds)]_{\text{exact}}}{[(1/p_\infty)(dp/ds)]_{TC}}$$

is plotted as a function of K_c for $\gamma = 1.40$ in Fig. 6a. The exact values of $(1/\kappa) \times (1/p_\infty)(dp/ds)$ have been calculated by Cabannes[33] for K_c up to about 0.70. For $K_c > 1.5$ the values obtained by Van Dyke[29] were employed and a curve faired between these calculations in the intermediate range. The exact limiting value of $(1/\kappa)(1/p_\infty)(dp/ds)$ as $K_c \to \infty$ is extremely close to the Newtonian approximation plus centrifugal force for all γ in the range $1 \leq \gamma \leq 5/3$—i.e.,

$$[(1/\kappa)(1/p_\infty)(dp/ds)]_{\text{exact}} \to 2.5\gamma M_\infty^2\theta_c$$

But $$\left(\frac{1}{\kappa}\frac{1}{p_\infty}\frac{dp}{ds}\right)_{TC} \to \frac{2\gamma(\gamma + 7)(\gamma + 1)}{(\gamma + 3)^2} M_\infty^2\theta_0 \qquad \text{as } K_c \to \infty$$

so that $$\lambda_{TC} \to (5/4)\{(\gamma + 3)^2/[(\gamma + 7)(\gamma + 1)]\}$$

This limiting value of λ_{TC} is plotted as a function of λ in Fig. 6b.

Recently Probstein and Bray[34] applied the tangent-cone approximation to unyawed slender bodies of revolution. By utilizing Eq. (7) for the pressure for $K_c \geqq 1$ and the von Kármán relation for $K_c < 1$, they were able to obtain relatively simple algebraic expressions for the pressure distribution and the drag coefficient for circular-arc ogives as functions of $K = M_\infty/(l/d)$ over practically the entire range of supersonic speeds. When their calculations are compared with rotational characteristics solutions, the agreement is excellent.

(2.2) Newtonian Approximation

So much has been written about the Newtonian approximation that we will discuss only the main points here.

For slender airfoils and bodies of revolution, the centrifugal force correction seems to improve the accuracy of the approximation. As shown in references 10–12,

$C_p = 2(\theta^2 + z\kappa)$ for slender airfoils

$C_p = 2\theta^2 + r\kappa$ for slender bodies of revolution

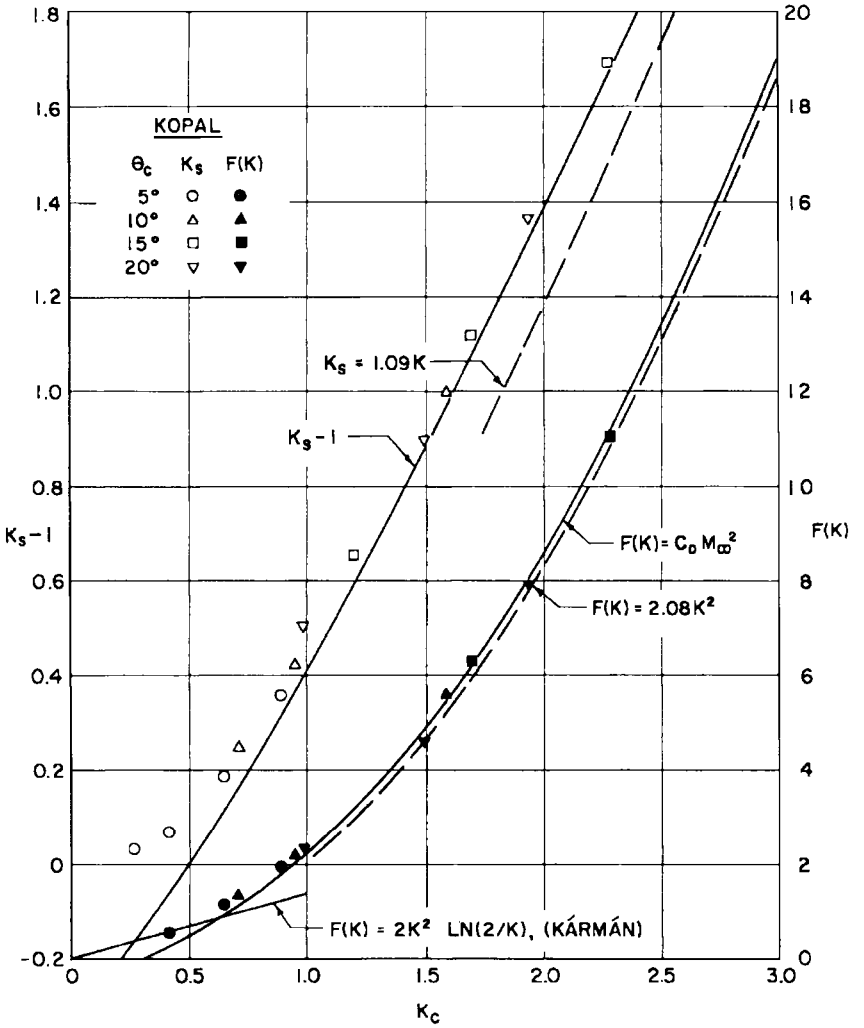

FIG. 5. Conical shock angle parameter $K_s = M_\infty \theta_s$ and drag function $F(K) = C_D M_\infty{}^2$ vs. similarity parameter $K_c = M_\infty \theta_c$.

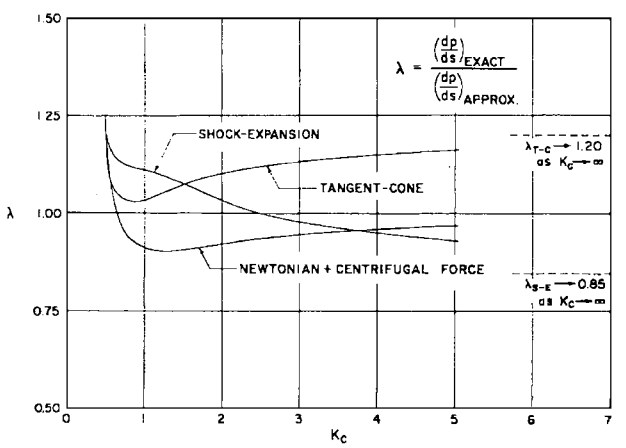

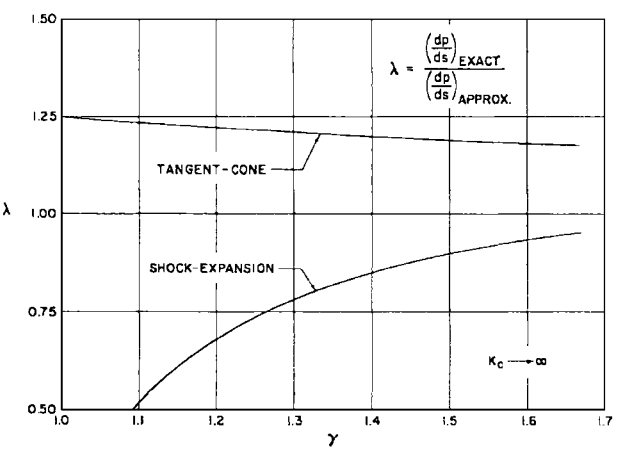

FIG. 6a (*left*). Initial pressure gradient ratio on ogive of revolution—hypersonic approximations $\gamma = 1.40$. FIG. 6b (*right*). Limiting values of initial pressure gradient ratio on ogive of revolution.

It is characteristic of the Newtonian approximation that all aerodynamic coefficients are independent of the flight Mach Number, and this statement is certainly correct for $M_\infty > 10$ for slender bodies and at much lower Mach Numbers for blunt bodies.

The Newtonian approximation says nothing about the portion of the body in the "shadow" of the flow. Since inviscid theory states that the pressure on the shielded portion of the body lies between 0 and p_∞, the pressure coefficient lies in the range $-2/\gamma M_\infty^2 \leq C_p \leq 0$, and these portions of the surface make a negligible contribution to aerodynamic properties at high Mach Numbers. When viscous effects are taken into account, it is probable that $p > p_\infty$ because of boundary-layer break-away caused by "feedback" of the pressure rise from the rear of the body or from the wake.

The Newtonian expressions for C_p are to be compared with the limiting values

$$\left.\begin{aligned} C_p &\to (\gamma + 1)\theta_w^2 && \text{for a wedge} \\ C_p &\to [2(\gamma + 1)(\gamma + 7)]/(\gamma + 3)^2\,\theta_c^2 && \text{for a cone} \end{aligned}\right\} \text{as } K \to \infty$$

For airfoils the Newtonian pressures are too low even in the limit $K_w \to \infty$. The initial pressure gradient on a plane ogive is given by

$$[(1/\kappa)(1/p_\infty)(dp/ds)]_{\text{N.+C.F.}} = 3\gamma M_\infty^2 \theta_w$$

so that $$\lambda_{\text{N.+C.F.}} \to [\gamma(\gamma + 1)]/[2(2\gamma - 1)] \qquad \text{for } K_w \to \infty$$

Of course $\lambda_{\text{N.+C.F.}} \to 1$ as $\gamma \to 1$ and $K_w \to \infty$, but the initial pressure gradient is very close to the exact value for *all* γ in the range $1 \leq \gamma \leq 5/3$ (Fig. 3b).

For the unyawed cone, the exact limiting value of C_p for $K_c \to \infty$ is very close to the Newtonian value—for example, $C_p \to 2.08\ \theta_c^2$ for $\gamma = 1.40$. The initial pressure gradient on an ogive of revolution is practically identical with the exact value. Thus the Newtonian approximation is particularly useful for hypersonic flows over slender bodies of revolution (Fig. 6a).

As an example of the results to be expected of the Newtonian approximation in a particular case, values of the pressure coefficients over a yawed circular cone of 10° half-angle will be compared with experimental values obtained at $M = 6.86$ and with Ferri's[35] theory. In this case $\cos\sigma = (\cos\alpha \sin\theta_c - \sin\alpha \cos\theta_c \cos\phi)$, where σ is the angle between the normal to a surface element and the flight direction, α is angle of yaw, θ_c is cone half-angle, and ϕ is the polar angle in a plane transverse to the cone axis measured from the most leeward ray. The simple relation $C_p = 2\cos^2\sigma$ is used here. Beyond the point at which $\sigma = \pi/2$, $C_p = 0$.

In Fig. 7 the calculated and experimental angular distributions of pressure coefficient are shown for angles of attack of 6.7° and 14°. Clearly the simple Newtonian approximation is quite adequate in this case, and any deviations are probably caused by viscous cross-flow effects on the leeward side.

(2.3) *Shock-Expansion Method*

It is remarkable that the Prandtl-Meyer relation based on local pressure and Mach Number behind the leading edge or bow shock furnishes a highly accurate approximation to the $p - \theta$ field for γ not too close to unity. As Eggers and Syvertson[15] have shown, the expansion waves from the body surface are largely

absorbed by the shock wave, except near shock detachment. A measure of the strength of the reflected waves is the ratio of the rate of variation of flow angle along Mach waves emanating from the surface, $\partial\theta/\partial c_1$, to the rate of variation, $\partial\theta/\partial c_2$, along the reflected waves. For the Prandtl-Meyer flow, $\partial\theta/\partial c_1$ is zero. Eggers and Syvertson find that the ratio $(\partial\theta/\partial c_1)(\partial\theta/\partial c_2)$ is never larger than 0.06 for $\gamma = 1.40$, so long as $\theta < 44°$ (approximately), even in the limiting case $M_\infty \to \infty$. This ratio rapidly increases in magnitude as $\gamma \to 1$, and the shock-expansion method becomes inaccurate. Such behavior is expected because the Mach Number just behind the shock approaches the value $(1/\theta_w)\sqrt{\{2/[\gamma(\gamma-1)]\}}$ as $K_w \to \infty$. As $\gamma \to 1$, the Prandtl-Meyer change in pressure for a given change in flow inclination becomes infinitely large compared with the change in pressure across an oblique shock wave; therefore, the reflected waves are nearly as strong as the waves from the body surface.

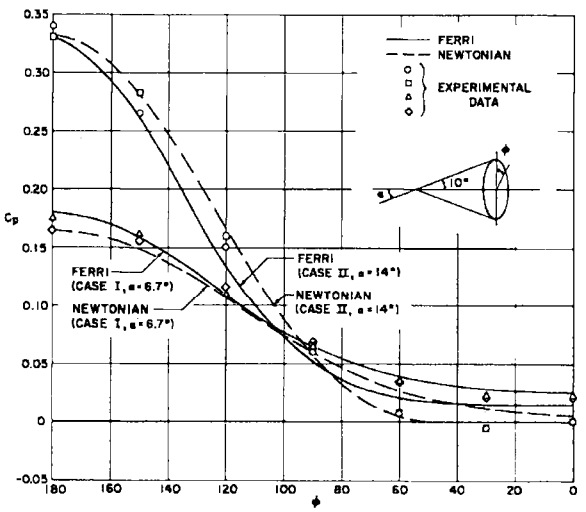

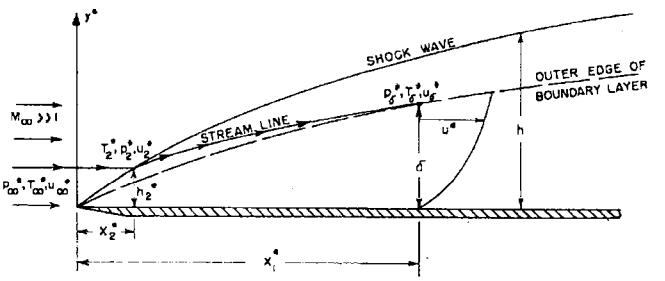

FIG. 7 (*left*). Comparison of experimental and calculated pressure distributions on yawed circular cone at $M = 6.86$. FIG. 8 (*right*). Hypersonic viscous flow over a flat plate.

Kraus[24] tabulated the value of

$$\lambda_{SE} = \frac{(dp/ds)_{\text{exact}}}{(dp/ds)_{SE}}$$

for $\gamma = 1.40$, and this ratio is shown as a function of K for various values of θ_w in Fig. 3a for comparison with the tangent-wedge approximation.† In the limit $K_w \to \infty$, the quantity

$$[(1/\kappa)(1/p_\infty)(dp/ds)]_{SE} \to \{[\gamma(\gamma+1)]/2\}\sqrt{2\gamma/(\gamma-1)}M_\infty{}^2\theta_w$$

therefore

$$\lambda_{SE} \to [3/(2\gamma-1)]\sqrt{[\gamma(\gamma-1)]/2}$$

This limiting value is plotted vs. γ in Fig. 3b. For $1 < \gamma < 1.2$, it appears that the Newtonian approximation is most suitable.

Even more surprising is the fact that the shock-expansion method is a good approximation for three-dimensional hypersonic flows. In order for this to be so,

† In Fig. 3a, $\delta_N = \theta_w$.

the flow must be locally two-dimensional—i.e., the rate of divergence of streamlines in planes tangent to the surface must be small compared with the rate of divergence of streamlines $\partial\theta/\partial z$ in planes normal to the surface. But $(\partial\theta/\partial z) = M(\partial\theta/\partial x) = M\kappa$, so that the lateral rate of divergence of the flow must be small compared with the product of local Mach Number and surface curvature in the stream direction. Evidently at high Mach Numbers this condition is satisfied for a wide class of flows—both steady and nonsteady. For such flows, the surface streamlines are practically coincident with the geodesics,† and the shock expansion method is applied in planes normal to the surface very much as in the case of an airfoil. In its *present form*, the shock-expansion method is obviously not applicable to bodies of zero curvature, such as cones or cone-cylinders, but here the tangent-cone or Newtonian approximations are available.

For a sharp-nosed unyawed body of revolution, the initial pressure gradient is $1/p_\infty(dp/ds) = \gamma\kappa M_c(p_c/p_\infty)$, according to the shock-expansion method, where (p_c/p_∞) and M_c are obtained from the Taylor-Maccoll values for an unyawed cone. The ratio $\lambda_{SE\text{ogive}}$ is plotted against K_c for $\gamma = 1.40$ in Fig. 6a. By utilizing Lees results,[31] one finds that

$$M_c \to (1/\theta_c)[(\gamma + 3)/(\sqrt{\gamma - 1}\,\sqrt{2\gamma^2 + 5\gamma + 1})] \qquad \text{as } K_c \to \infty$$

so that

$$\left(\frac{1}{\kappa}\frac{1}{p_\infty}\frac{dp}{ds}\right)_{SE\text{ogive}} \to \frac{\gamma^2(\gamma + 7)(\gamma + 1)}{(\gamma + 3)\sqrt{\gamma - 1}\,\sqrt{2\gamma^2 + 5\gamma + 1}} M_\infty\theta_c^2$$

therefore,

$$\lambda_{SE\text{ogive}} \to [(2.5)(\gamma + 3)]/[\gamma(\gamma + 7)(\gamma + 1)]\sqrt{\gamma - 1}\,\sqrt{2\gamma^2 + 5\gamma + 1}$$

This limiting value is shown as a function of γ in Fig. 6b.

(3) Hypersonic Viscous Flow over Slender Bodies

(3.1) Fluid-Mechanical Models

When the leading edge or nose of a slender body is sufficiently sharp,‡ one expects the concepts of hypersonic similarity and the hypersonic approximations to connect the self-induced flow field with the rate of boundary-layer growth. Two conceptually different methods have been employed to attack this problem:

(1) In Shen's[19] analysis, the static pressure $p(x)$ is regarded as constant across the whole flow between shock and body in the direction normal to the body surface and equal to its value just behind the oblique shock wave. Shen considers only strong shocks, for which

$$p(x)/p_\infty = [2\gamma/(\gamma + 1)]M_\infty^2(d\delta/dx)^2$$

† The fact that the streamlines are geodesics was established for the Newtonian approximation in reference 11.

‡ For the present a definition of the term "sharp" is carefully avoided; later we will attempt to give a more precise statement.

Here $\delta(x)$ is the height of the shock above the axis, and $(d\delta/dx)$ is the local shock angle with respect to the free-stream direction. He applies the von Kármán momentum integral method to the entire region between shock wave and body surface and obtains a second (integral) relation between $\delta(x)$ and $p(x)$. By representing the velocity profile $u/u_\infty\,(z)$ as a straight line $(u/u_\infty) = (z/\delta)$, and solving these two simultaneous equations approximately, Shen obtains the (correct) result that $\delta \sim x^{3/4}$ and $(p/p_\infty) \sim (1/\sqrt{x})$ on an insulated sharp-nosed flat plate at hypersonic speeds.

The present author[36] pointed out that this approach is inconsistent with the equation of continuity, but fortunately (as we shall see below) this inconsistency leads only to a difference in a numerical factor. Since the static pressure ratio p/p_∞

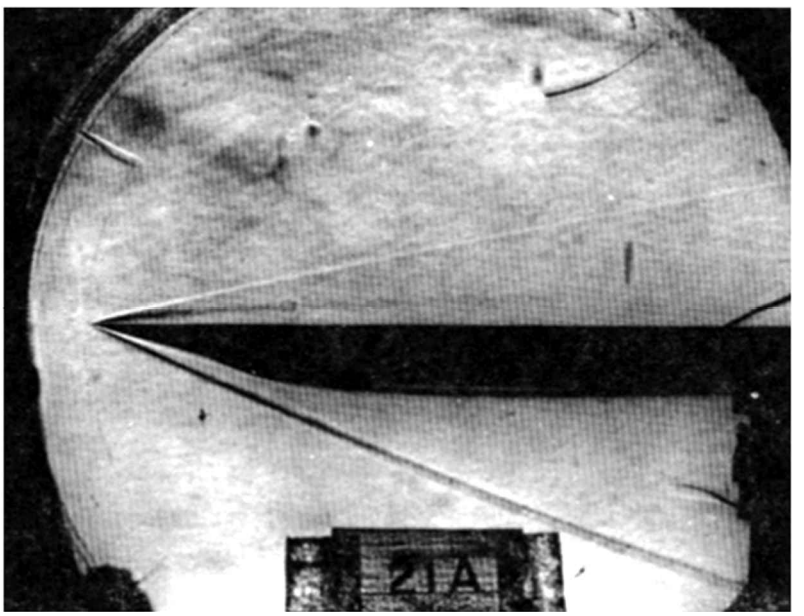

FIG. 9. Schlieren photograph of shock wave boundary-layer interaction on insulated plane surface at $M_\infty = 7.9$. Re per in. = 85,000 and $Re_t < 100$ (GALCIT).

is of order $M_\infty{}^2(\delta^2/x^2)$, the average density ratio $\bar{\rho}/\rho_\infty$ between shock wave and body surface in Shen's analysis is of order

$$\frac{p/p_\infty}{\bar{T}/T_\infty} \sim \frac{M_\infty{}^2(\delta^2/x^2)}{M_\infty{}^2} = \frac{\delta^2}{x^2}$$

Therefore, the mass flux ratio

$$\frac{\overline{m}}{\rho_\infty u_\infty \delta} = \int_0^1 \frac{\rho}{\rho_\infty}\frac{u}{u_\infty}\frac{dz}{\delta}$$

is also of order δ^2/x^2. But $\overline{m}$ must be equal to the mass flux across the height δ in the free stream ahead of the shock, so that $(\overline{m}/\rho_\infty u_\infty \delta) = 1$. As Dr. Hammitt has observed, in this approach the mass is conserved only if the shock wave is a straight line!

(2) In the second approach, adopted by Probstein and the present author,[36, 37, 38] this inconsistency at least is avoided, because the shock wave and the boundary

layer are regarded as distinct (Figs. 8 and 9). By the same argument used above, the mass flux ratio across the boundary layer is of order δ^2/x^2 and is small, except possibly near the leading edge. Therefore, the streamlines entering the boundary layer are very nearly parallel to the outer edge—i.e.,

$$\frac{(\theta - \theta_b) - (d\delta^*/dx)}{\theta - \theta_b} = 0(\delta^2/x^2)$$

or

$$\theta \cong \theta_b + (d\delta^*/dx) \cong \theta_b + (d\delta/dx)$$

[For a flat plate at zero angle of attack, $\theta_b = 0$ and $\theta \cong (d\delta/dx)$.] The static pressure at $z = \delta(x)$ is then related to θ, and therefore to $(d\delta/dx)$, by means of one of the accurate hypersonic approximations discussed in Section (2); the tangent-wedge (or tangent-cone) approximation is utilized because of its simplicity. A second relation between $p(x)$ and $\delta(x)$ is obtained from the Prandtl boundary-layer equations. Since $(1/T_\infty)(dT/dz) = 0(M_\infty{}^2)$ in the boundary layer, it is not difficult to show that the pressure gradients in the "external" inviscid flow do not penetrate very far into the boundary layer, but die out quickly in a "buffer layer" of thickness $\delta/M_\infty{}^2$. All of the usual Prandtl approximations are valid so long as δ^2/x^2 is small.

By continuity, a relatively dense cool gas layer must exist between the boundary layer and the shock wave. Viscous forces and heat conduction are of order δ^2/x^2 or smaller in this zone, and the flow is inviscid but contains vorticity because of the shock curvature. This external flow can be constructed by means of one of the hypersonic flow methods or by actually solving the rotational flow equations of motion, as Stewartson[39] has done for the case of "strong" interaction on a flat plate.

According to the tangent-wedge approximation $(p/p_\infty) \to \{[\gamma(\gamma+1)]/2\} M_\infty{}^2 \times (d\delta/dx)^2$ for a flat plate if $M_\infty{}^2(d\delta/dx)^2 \gg 1$. The results obtained by the two quite different methods (1) and (2) in this particular case will differ finally by a numerical factor of only $(\gamma + 1)/2$, if both are carried out correctly. This difference corresponds to the small pressure variation normal to the streamlines in hypersonic flow over a slender body, or, more precisely, to the fact that the shock angle,

$$\theta_s \to [(\gamma + 1)/2]\theta_w \qquad \text{as } K_w \to \infty$$

Nagamatsu and Li[40] extended Shen's analysis by approximating the velocity profile by a quartic, as in the usual Kármán-Pohhausen approach. Unfortunately they did not use the Howarth normal distance

$$Y = \int_0^z \frac{\rho}{\rho_\infty}\, dz$$

so that an additional numerical factor appeared. As expected, when the momentum integral method is carried out in Howarth coordinates utilizing the TW relation, the results[39] agree within 2 per cent with those obtained by the present author[36] from the solutions of the boundary-layer equations.

The approach utilized by Shen is obviously not applicable to "weak" interactions, while the method adopted by Probstein and the present author is quite general. Therefore, our subsequent discussion is limited to the main aspects and results of this second approach.

(3.2) *Strong and Weak Interactions*

The solutions of the Prandtl boundary-layer equations must match the velocity, vorticity, and stagnation enthalpy of the "external" inviscid flow at the "outer edge" of the boundary layer. For isoenergetic flows, the "external" stagnation enthalpy is a known constant equal to its free-stream value. The quantities u_δ and $(\partial u/\partial z)_\delta$ depend not only on the local pressure, but also on the streamline trajectories and shock wave curvature, which are unknown a priori. Lees[41] shows that this circle is broken by considering first the limiting case $M_\infty \to \infty$, with the hypersonic viscous interaction parameter

$$\bar{\chi}_\infty = (M_\infty{}^3 \sqrt{C})/\sqrt{Re_x}$$

held fixed. In the strong interaction region, where $\chi_\infty \gg 1$, $u_\delta \to u_\infty$ and $(\partial u/\partial z)_\delta \to 0$ in this limiting case, while in the weak interaction region $(\partial u/\partial z)_\delta \to 0$ and u_δ is connected with p_δ by the Bernoulli relation.

Suppose that we consider planar flows first and then extend the results to the unyawed cone as an example of three-dimensional flows. According to the tangent-wedge approximation, $p(x)$ and $d\delta/dx$ are connected by Eq. (4a), Section (2.1), or

$$p/p_\infty = 1 + \{[\gamma(\gamma+1)]/4\}K^2 + \gamma K\sqrt{1 + [(\gamma+1)/4]^2K^2} \qquad (4a)$$

where $$K = M_\infty\theta_b + M_\infty(d\delta/dx)$$

In the "inverse" problem, $p(x)$ is prescribed and Eq. (4a) furnishes a relation between the unknowns $\theta_b(x)$ and $(d\delta/dx)$. The boundary-layer thickness distribution is obtained by the von Kármán momentum integral method, and the required airfoil shape $\theta_b(x)$ can then be computed. At the suggestion of Tsien, such calculations have been carried out by Ting-Yi Li and the present author.†

In order to bring out the major aspects and important parameters of hypersonic viscous interaction, the "direct" problem is discussed for the inclined wedge (or flat plate), where $\theta_b = \text{const.} = \theta_w \pm \alpha$, and the problem is greatly simplified.

(A) *Strong Interaction.*—The strong interaction region is characterized by the fact that

$$(d\delta/dx) > \theta_b \text{ and } K = M_\infty\theta = [M_\infty(\theta_w \pm \alpha) + M_\infty(d\delta/dx)] \gg 1$$

This interaction is important for sharp-nosed airfoils at not too high angles of attack, when the Mach Number is sufficiently high and the Reynolds Number is sufficiently low. By Eq. (4a), $p/p_\infty \to \{[\gamma(\gamma+1)]/2\}M_\infty{}^2\theta^2$ in this case, and the viscous interaction problem is essentially nonlinear. On a flat plate at zero angle of attack, for example,

$$\delta^2 \sim \frac{\mu/\mu_\infty}{\bar{\rho}/\rho_\infty} \cdot \frac{\nu_\infty x}{u_\infty} \sim \frac{C(\bar{T}/T_\infty)^2}{p_\delta/p_\infty}\frac{\nu_\infty x}{u_\infty}$$

when μ/μ_∞ is approximated by $C(\bar{T}/T_\infty)$, where C—the Chapman-Rubesin viscosity factor—equals $[(\mu_w/\mu_\infty)/(T_w/T_\infty)]$. Since $(\bar{T}/T_\infty) \sim M_\infty{}^2$, we have

$$\delta^2 \sim [CM_\infty{}^4/(p_\delta/p_\infty)]\cdot(\nu_\infty x/u_\infty)$$

† To be published soon.

while $p_\delta/p_\infty \sim M_\infty{}^2(\delta^2/x^2)$ according to *TW*. By combining these two estimates, one finds that

$$p_\delta{}^{(0)}/p_\infty = p_0[(M_\infty{}^3\sqrt{\bar{C}})/\sqrt{Re_x}] = p_0\bar{\chi}_\infty$$

$$(\delta^{(0)}/x) = \delta_0 C^{1/4}[\sqrt{M_\infty}/(Re_x)^{1/4}] = \delta_0(\sqrt{\bar{\chi}_\infty}/M_\infty)$$

The condition $K \gg 1$ means that $\bar{\chi}_\infty \gg 1$.†

For the case of strong interaction on an inclined wedge, Eq. (4a) takes the form of the following asymptotic expansion:[42]

$$\frac{p}{p_\infty} = \frac{\gamma(\gamma+1)}{2} M_\infty{}^2\left(\frac{d\delta}{dx}\right)^2\left[1+\frac{\theta_b}{(d\delta/dx)}\right]^2 + \frac{3\gamma+1}{\gamma+1} - \frac{8\gamma}{(\gamma+1)^3}\frac{1}{M_\infty{}^2(d\delta/dx)^2}\frac{1}{\{1+[\theta_b/(d\delta/dx)]\}^2} + \ldots \quad (8)$$

The zeroth approximation to the strong interaction on a flat-plate suggests that the generating parameter for the wedge is

$$(M_\infty\theta_b)/[M_\infty(d\delta/dx)] \sim K_b/\sqrt{\bar{\chi}_\infty}$$

and the pressure can be represented by an asymptotic series expansion of the form

$$p/p_\infty = p_0\bar{\chi}_\infty\{1 + [(p_1K_b)/\bar{\chi}_\infty{}^{1/2}] + [(p_2 + p_3K_b{}^2)/\bar{\chi}_\infty] + \ldots\} = p_0\cdot\bar{\chi}_\infty B_1 \ddagger \quad (9)$$

$$p/p_\infty = p_0\bar{\chi}_\infty + p_2 + 0(1/\bar{\chi}_\infty)$$

The quantity $(\delta/x)[Re_x{}^{1/4}/(C^{1/4}\sqrt{M_\infty})](1/\delta_0)$ is expanded in an asymptotic series similar to B_1, and the δ_j's are related to the p_j's by means of Eqs. (8) and (9)—i.e., only one set of independent constants remains, and these constants are to be determined from the solutions of the Prandtl boundary-layer equations. Analytical solutions of these equations for velocity and stagnation enthalpy are sought as asymptotic series expansions of the form

$$\omega(x,y) = \omega_0(\eta_i) + (K_b/\bar{\chi}_\infty{}^{1/2})\omega_1(\eta_i) + \{[\omega_2(\eta_i) + K_b{}^2\omega_3(\eta_i)]/\bar{\chi}_\infty] + \ldots$$

where $\eta_i \sim (y/x)[Re_x{}^{1/4}/(C^{1/4}M_\infty{}^{1/2})]$, and $\omega_0(\eta_i)$ and $H_0(\eta_i)$ are the solutions for the case of a surface parallel to the flight direction ($K_b = 0$). The functions $\omega_1(\eta_i)$, $H_1(\eta_i)$, etc., satisfy linear ordinary second-order differential equations with coefficients depending only on the previous terms in the expansion. The local skin-friction and heat-transfer coefficients are also expressed as asymptotic series, of the form

$$C_f = \tilde{C}_f\sqrt{[p^{(0)}/p_\infty]/2}\{1 + (a_1K_b/\bar{\chi}_\infty{}^{1/2}) + [(a_2 + a_3K_b{}^2)/\bar{\chi}_\infty] + \ldots\}$$

where $\tilde{C}_f$ is the "classical" value of $0.664\sqrt{\bar{C}}/\sqrt{Re_x}$.

For strong interaction, the major effect of the pressure is to contract the scale of distance normal to the surface by a factor, $\sim\sqrt{p/p_\infty}$, and thereby increase the local skin-friction and heat-transfer coefficients by the same factor. It should be

† Of course these rough considerations are supported by detailed analysis.

‡ For the flat plate at zero angle of attack

noted that the expression for C_f is integrable and the total skin-friction drag in the strong interaction region is finite. Also the self-induced pressure-drag, lift, and moments are all finite.

Although the details[36, 38, 42] cannot be given here, the basic case of the surface parallel to the oncoming stream is particularly simple. The differential equations for velocity $w_0(\eta_i)$ and stagnation enthalpy $H_0(\eta_i)$ are identical with the boundary-layer equations for the "similar solutions" in the limit $M_\infty \to \infty$ considered recently by Levy,[43] with β, the pressure gradient parameter, equal to $[(\gamma - 1)/\gamma]$.† In the special case $Pr = 1$, these equations reduce to the low-speed boundary-layer equations with heat transfer for an "external" velocity distribution of the form $u_\delta \sim x^m$, where $\beta = [2m/(m + 1)]$. The numerical solutions of these simpler equations have been studied extensively by Cohen and Reshotko,[44] and Li and Nagamastu.[45, 46] In the doubly special case of no heat transfer and $Pr = 1$, Crocco found that $H_0 = 1$; therefore, in this case,[36] the momentum equation is identical with the well-known Falkner-Skan equation.[47, 48]

For our problem, the constant p_0 in the expression for the induced pressure $p = p_0\bar{\chi}_\infty$ is given by

$$p_0 = (9/32)\gamma(\gamma + 1)\delta_0^2 = (3/8)\sqrt{\gamma(\gamma + 1)}\,(\gamma - 1)G[(T_w/T_{s_\infty}), Pr]_{\beta = \frac{\gamma-1}{\gamma}}$$

where $$G\left(\frac{T_w}{T_{s_\infty}}, Pr\right)_{\beta = \frac{\gamma-1}{\gamma}} = \sqrt{2}\int_0^\infty (H_0 - w_0^2)\,d\eta_i$$

so that $$C_f = (\sqrt{3}/2\sqrt{2})[\gamma(\gamma + 1)]^{1/4}\sqrt{\gamma - 1} \times \sqrt{G}\,(dw_0/d\eta_i)_{\eta i = 0}[(M_\infty^{3/2}C^{3/4})/(Re_x)^{3/4}]$$

with a similar expression for C_H. For $Pr = 1.0$, the values of $(dw_0/d\eta_i)_{\eta i = 0} \equiv K''(0) \equiv f_w''$ for $\beta = (\gamma - 1)/\gamma$ are obtained from Fig. 1 of reference 46, or Fig. 6 of reference 44, for values of T_w/T_{s_∞} of 0, 0.2, 0.6, 1.0, and 2.0. Other values may be found by interpolation. Similarly, values of $(dH_0/d\eta_i)_{\eta i = 0} \equiv S_w'$ for $Pr = 1$ and $\beta = (\gamma - 1)/\gamma$ are obtained from Fig. 8 of reference 44. The quantity G would have to be determined by integrating the tabulated functions f' and $S + 1$; such calculations are being carried out by Ting-Yi Li and Nagamatsu.

Two special cases may be noted briefly.

(i) *Zero heat transfer and* $Pr = 1$: In this case

$$G = \sqrt{2}\int_0^\infty [(1 - w_0) + (w_0 - w_0^2)]d\eta_i = \left[\delta^*\sqrt{\frac{u_\infty}{\nu_\infty x}} + \delta^{**}\sqrt{\frac{u_\infty}{\nu_\infty x}}\right]_{\beta = \frac{\gamma-1}{\gamma}}$$

where the quantity in brackets is the sum of the nondimensionalized displacement and momentum thicknesses for the Falkner-Skan profile. For air, $\gamma = 1.40$, $\beta = 0.286$, and $G = 1.88$, $(dw_0/d\eta_i)_{\eta i = 0} = 0.765$. Here $(p^{(0)}/p_\infty) = 0.52\,\bar{\chi}_\infty$, $(\delta^{(0)}/x) = 0.74[(C^{1/4}M_\infty^{1/2})/Re_x^{1/4}]$ and $C_f = 0.55[(M_\infty^{3/2}C^{3/4})/Re_x^{3/4}]$, as compared with the "classical" value $\tilde{C}_f = (0.664\sqrt{C}/Re_x^{1/2})$.

† Unfortunately the solutions for w_0 and H_0 are not tabulated in Levy's paper.

(ii) *Large heat transfer:* When the surface temperature is much lower than equilibrium temperature, as in free flight problems, the direct effect of pressure gradient is small compared to the thermodynamic effect, and a good approximation is obtained by dropping the pressure gradient term.[36] In that case, $\omega_0(\eta_i)$ satisfies the Blasius equation for *any value of the Prandtl Number,*† and the solution for $H_0(\eta_i)$ is then identical with the solution found by Crocco[49] for arbitrary Prandtl Number and zero pressure gradient. For our problem, $G(Pr) = 2\sqrt{2}\int_0^\infty \theta_{pr}{}^{II}(\omega_B)d\eta_B$,‡ and $G(1) = 0.664$, $G(0.725) = 0.580$. For air with $Pr = 0.725$, $p^{(0)}/p_\infty = 0.16\,\bar{\chi}_\infty$, $(\delta^{(0)}/x) = 0.41[(C^{1/4}M_\infty{}^{1/2})/Re_x{}^{1/4}]$, and $C_f{}^{(0)} = 0.19[(M_\infty{}^{3/2}C^{3/4})/Re_x{}^{3/4}]$, while $C_H{}^{(0)} \cong 0.45C_f{}^{(0)}$. Thus the self-induced effects are much smaller in the highly cooled case, as expected, because the maximum boundary-layer temperature is much lower. However, the differences between this case and the insulated surface are not quite as large as they appear at first because $C < 1$ for a insulated surface while $C \cong 1$ for the highly cooled case.

(*b*) *Weak Interaction.*—In the weak interaction region, the self-induced pressure field is essentially a perturbation on the original uniform inviscid wedge (or cone) flow. *Either* $(d\delta/dx) < \theta_b$ with $M_\infty\theta_b$ arbitrary, *or* $M_\infty\theta \leq 1$ and $d\delta/dx$ may be either larger or smaller than θ_b. Weak interaction effects appear on thin wedges at low angles of attack when the Reynolds Number is high or the Mach Number is only moderately supersonic, and also at high Mach Numbers on thick wedges or on the compression surface of any wedge at high angles of attack. Along the curve $z = \delta(x)$, the pressure is expressed as a Taylor series expansion as follows:

$$p = p_b\left[1 + \frac{1}{p_b/p_\infty}\left(\frac{dp/p_\infty}{d\theta}\right)_{\theta=\theta_b}(\theta - \theta_b) + \frac{1}{2!}\frac{1}{p_b/p_\infty}\left(\frac{d^2p/p_\infty}{d\theta^2}\right)_{\theta=\theta_b}(\theta - \theta_b)^2 + \ldots\right]$$

where p_b is the inviscid wedge pressure given by Eq. (4a), and $[(1/p_\infty)(dp/d\theta)]_{\theta=\theta_b}$ is given by Eq. (5), Section (2.1). Of course, $\theta - \theta_b = d\delta/dx$. The iteration scheme logically begins by taking $d\delta/dx$ equal to the expression obtained from the usual boundary-layer solution for zero pressure gradient on the wedge—i.e.,

$$d\delta/dx \cong d\delta^*/dx = d_b\sqrt{C_b}(M_b{}^2/\sqrt{Re_{x_b}})$$

where $d_b = (T_w/M_b{}^2)\cdot A(Pr) + (\gamma - 1)\cdot B(Pr)$ (noninsulated)

$d_b = D(\gamma - 1)$ [insulated; $D = B + (A/2)$]

For $Pr = 1$, $A = 0.865$, $B = 0.166$, and $D = 0.599 \cong 0.60$, while for $Pr = 0.725$, $A = 0.968$, $B = 0.145$, and $D = 0.556$. By combining all these expressions one obtains

$$p/p_b = 1 + \gamma F_b\bar{\chi}_b + 0(F_b{}^2\bar{\chi}_b{}^2)$$

† This procedure may be applied to good advantage in many heat-transfer problems where $T_w \ll T_{s\infty}$.

‡ $\theta_{Pr}{}^{II}\omega_B$) is the enthalpy-velocity function introduced by Crocco.[49]

where
$$F_b = d_b \frac{K}{K_b} \frac{[(1/M_\infty)(1/p_\infty)(dp/d\theta)]_{\theta=\theta_b}}{p_b/p_\infty}$$
$$\bar{\chi}_b = (M_b^3 \sqrt{C_b})/\sqrt{Re_{xb}}, \text{ etc.}\dagger$$

In the particular case of a thick wedge or on the compression side of a wedge at high angle of attack such that $M_\infty\theta_b > 2$, then

$$F_b \to (2/\gamma K_b)d_b$$
$$p/p_b = 1 + (2d_b/K_b)\chi_b + \ldots$$

But $M_b\theta_b \to \sqrt{2/[\gamma(\gamma-1)]}$ in this case, so that

$$\bar{x}_b/K_b = (\sqrt{C_b}M_b^2)/(\theta_b\sqrt{Re_{xb}}) \to (\sqrt{C}M_\infty)/(\theta_b^2\sqrt{Re_x}) = \bar{\chi}_\infty/K^2$$
$$p/p_b = 1 + (2d_b/K^2)\bar{\chi}_\infty + \ldots$$

Viscous interaction effects are reduced considerably in this case, as compared with the flat plate at zero angle of attack, because of the presence of a strong inviscid pressure field, as indicated by the factor $2/K^2$.

So far as the present author is aware the weak interaction self-induced pressure distribution on an insulated flat plate parallel to the oncoming stream was first obtained experimentally and theoretically by the research group in the NACA Langley 11 by 11 in. hypersonic tunnel, as reported by Becker.[50] An independent estimate was also made by Donaldson (unpublished). For this particular case

$$F_b = d_\infty = D(\gamma-1), \quad \text{and} \quad p/p_\infty = 1 + \gamma(\gamma-1)D\bar{\chi}_\infty + \ldots$$

The first-order perturbation on the velocity and enthalpy distributions for the flat plate was worked out by Probstein and the present writer,[37] and independently by Maslen.[51] Later the analysis was extended to the case of an inclined wedge.[38] Weak interactions were also considered by Bertram.[52] It seems quite natural to seek asymptotic series solutions of the form

$$u/u_b = \omega(x_1y) = \omega_0(\eta_i) + \bar{\chi}_b\omega_1(\eta_i) + \ldots$$

where now $\eta_i \sim (y/x)\sqrt{Re_{xb}}$, and $\omega_0(\eta_i)$ and $H_0(\eta_i)$ are the classical solutions for zero pressure gradient. By substituting the asymptotic series expansions for velocity and enthalpy into the boundary-layer equations a set of linear ordinary second-order differential equations for $\omega_1(\eta_i)$, $H_1(\eta_i)$, etc., is obtained in which the coefficients depend on the preceding terms in the expansion. The local skin-friction and heat-transfer coefficients and recovery factor are also obtained as series in $\bar{\chi}_b$.

To a first approximation (terms of order $\bar{\chi}_b$), it is found that the local heat-transfer coefficient and recovery factor are unaffected by the self-induced pressure gradient for any value of Pr. The increase in skin friction coefficient is small, but not negligible, and the velocity and temperature profiles are considerably altered.

In principle, the treatment of weak interaction outlined here is applicable to arbitrary three-dimensional flows. As an example, the case of the unyawed circular cone is analyzed by Probstein and Elliott,[53] and also by Lin, Schaaf, and Sherman,[54]

† $K = M_\infty\theta_b$; $K_b = M_b\theta_b$; $C_b = (\mu_w/\mu_b)/(T_w/T_b)$.

and by Talbot.[55] The discussion parallels that for the wedge step-by-step, except that the tangent-cone approximation is utilized. For $K = [M_\infty\theta_c + M_\infty(d\delta/dx)] > 1$, the inviscid pressure ratio p_c/p_∞ and $[(1/p_\infty)(dp/d\theta)]_{\theta=\theta_c}$ are given by Eqs. (6) and (7), Section (2.1). According to the Mangler transformation,

$$d\delta/dx = (d_c/\sqrt{3})\sqrt{C_c}(M_c^2/\sqrt{Re_{x_c}})$$

for an unyawed cone, so that

$$p/p_c = 1 + \gamma F_c\bar{\chi}_c + 0(F_c^2\bar{\chi}_c^2)$$

where

$$F_c = d_c(K/K_c)\tilde{F}_c(K_c;\ \gamma)$$

For $K \ll 1$, the Kármán-Moore slender body approximation is available for evaluating F_c. In the intermediate region $K = 0(1)$, the use of the slender body value of p_c/p_∞ can introduce errors that are larger than the entire induced pressure effect. Talbot's[55] calculation is open to criticism on this account. The inviscid cone pressure should be evaluated from exact Taylor-Maccoll theory in such cases.

When the reduced boundary-layer thickness in Howarth coordinates $\tilde{\delta} = \int_0^\delta \frac{\rho}{\rho_\infty}\,dz$ is no longer small compared with the radius of the body cross section, the effect of transverse curvature must be taken into account. Probstein and Elliott[56] find that the transverse curvature increases the local skin-friction coefficient, but hardly affects the boundary-layer displacement thickness, so that the effects of induced pressure and transverse curvature are separable, at least for $(\tilde{\delta}/r) = 0(1)$.

An entirely different approach to this whole problem is employed by Kuo,[56a] who extends Lighthill's method for "rendering solutions uniformly valid" to boundary-layer problems. For $\bar{\chi}_\infty < 1$, Kuo's results reduce identically to those obtained by the weak interaction theory described here. The present author would prefer to postpone discussion of the extension to large $\bar{\chi}_\infty$ until a published version of Kuo's work appears.

(3.3) Comparison Between Theory and Experiment: Influence of the Leading Edge at Hypersonic Speeds

Although the results are in some respects preliminary, enough experimental data are now available on hypersonic viscous interaction effects to permit some comparisons to be made with the "sharp" leading-edge theory described in Sections (3.1) and (3.2). Two sets of data on induced pressure are presented in Fig. 10 and 10a:

(1) static pressure distributions along the side of an insulated 20° wedge-probe parallel to the oncoming stream, obtained by Bertram[57] in the NACA Langley 11 by 11 in. hypersonic tunnel at $M = 6.86$, at a constant free-stream pressure corresponding to $Re_x/\text{in.} = 2.50 \times 10^5$. The various thicknesses of the blunt leading edge were obtained by taking a plane cut normal to the test surface. Here $370 \leq Re_t \leq 1960$.†

(2) similar data obtained by Kendall and Nagamatsu on an insulated flat plate

† Here Re_t is free-stream Reynolds Number based on leading-edge thickness (or diameter).

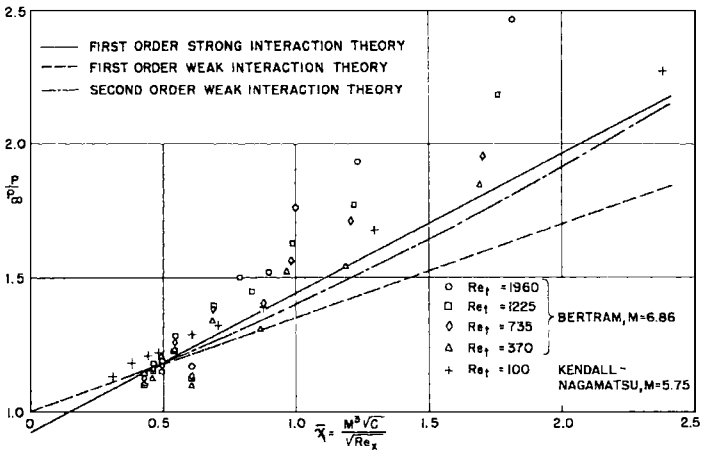

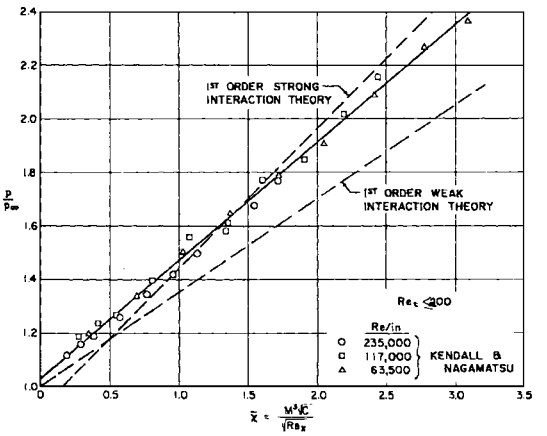

FIG. 10 (*left*). Induced pressure on a flat plate at hypersonic speeds. FIG. 10a (*right*). Induced pressure on a flat plate at $M = 5.8$.

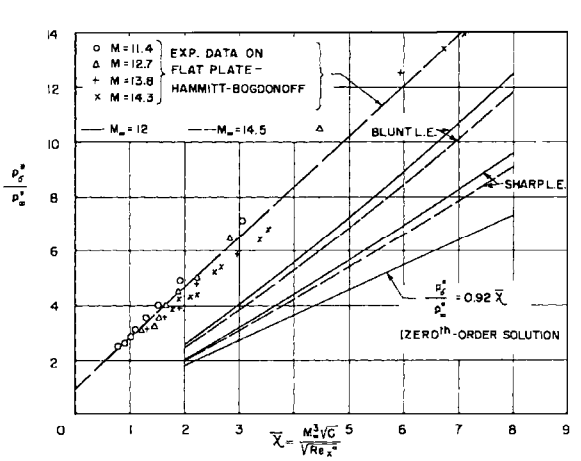

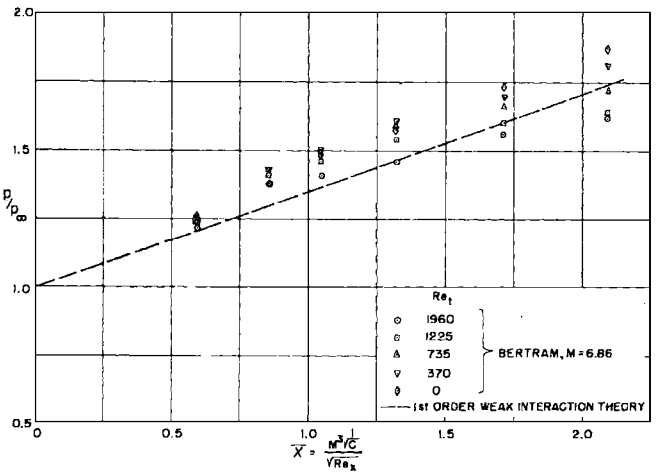

FIG. 11 (*left*). First-order effect of temperature rise and vorticity generated by leading-edge shock wave on induced pressures over insulated flat plate in helium. FIG. 12 (*right*). Induced pressures on a flat surface with effect of inviscid rotational flow subtracted.

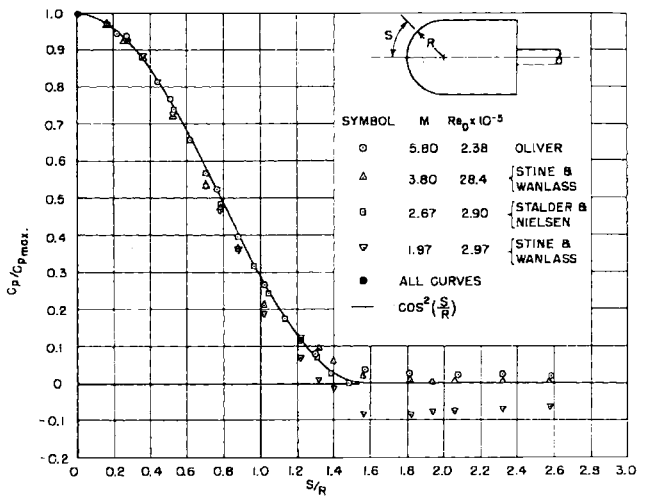

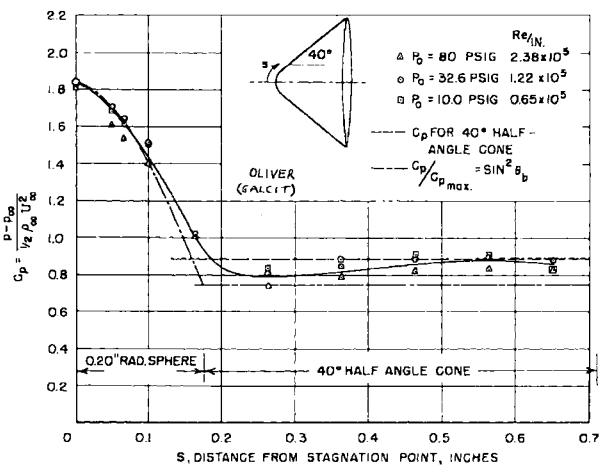

FIG. 13 (*left*). Pressure coefficient distribution on surface of hemisphere-cylinder at various Mach Numbers. FIG. 14 (*right*). Pressure distribution over blunt cone, $M_\infty = 5.8$, $\alpha = 0°$.

in the GALCIT 5 by 5 in. hypersonic tunnel at $M = 5.8$. The leading-edge thickness is about 0.001 in., or $Re_t \leq 200$.

Also shown in Fig. 10 and 10a are the linear and second-order weak interaction theory described by the relations

$$(p^{(1)}/p_\infty) = 1 + 0.35\bar{\chi}_\infty$$

$$(p^{(2)}/p_\infty) = 1 + 0.35\bar{\chi}_\infty + 0.05\bar{\chi}_\infty^2$$

and the strong interaction theory, given by $p/p_\infty = 0.52\ \bar{\chi}_\infty + 0.92$.† In this range, there is very little difference between the second-order weak interaction and the strong interaction predictions.

Kendall's data for $Re_t \leq 200$ and Bertram's data for $Re_t = 370$ are in close agreement with the theory. Kendall's results in particular are supported by detailed measurements of total head distribution between the shock wave and the plate surface at numerous stations, measurements of shock-wave shape, etc., all of which confirm the correctness of the fluid-mechanical model for the "sharp" leading edge. But in Bertram's experiments, the influence of the leading edge is already important for $Re_t = 735$, and for $Re_t = 1225$ this influence is dominant. An even more striking demonstration of the strong influence of the leading edge at hypersonic speeds is shown by the induced pressure measurements of Hammitt and Bogdonoff[58] obtained on a flat surface in the Princeton helium tunnel in the range $11.4 \leq M \leq 14.3$, with $\mathrm{Re}_t \cong 1000$ (Fig. 11). More recent measurements in this tunnel over a wide range of leading-edge thicknesses have shown that the qualitative behavior of the flow field is quite different for blunt and sharp leading-edges.

Two principal effects of the leading-edge region are currently being investigated:

(1) effect on the boundary layer of vorticity and temperature rise generated by the leading-edge shock;

(2) inviscid-flow effects associated with reflected waves from the strong, detached bow wave.

Lees[41] carried out an approximate calculation of the first effect which showed that the reduction in mass flux in the wake of the detached shock ("blanketing effect") could have an important influence on the boundary-layer displacement thickness and induced pressures. The results of this calculation are shown by the curves labelled "blunt" and "sharp" leading edge in Fig. 11. The large induced pressures observed for moderate $\bar{\chi}_\infty$ values are not explained by this study.

An approximate calculation of the reflected waves was made by Bertram,[57] who replaced the actual leading edge by a wedge of half-angle sufficient to give $M = 1$ behind the shock ($\theta_w = 43°$ at $M = 6.8$), followed by a sudden expansion to a surface parallel to the oncoming stream. At high Mach Numbers, the static pressure after such an expansion is still considerably higher than free-stream pressure. In fact, for $\gamma = 1.40$, the pressure ratio p_3/p_2 across a 43° Prandtl-Meyer expansion starting at $M = 1$ is 0.085, while the pressure ratio p_2/p_∞ across an oblique shock with $\theta_w = 43°$ is 44.6 at $M = 6.86$, so that $p_3/p_\infty = 3.8$. Evidently this ratio p_3/p_∞

† The coefficient 0.52 is derived in Section (3.2); the constant term is obtained from a solution of the von Kármán integral equation.

increases very nearly as $M_\infty{}^2$ for a fixed geometry. For this reason expansion waves of considerable total strength must be reflected from the leading-edge shock wave.† This conclusion is supported by the inviscid pressure distribution on the flat surface calculated graphically by Bertram as a function of x/t (Fig. 1 of reference 57). We shall follow a procedure that is the reverse of Bertram's and subtract the "inviscid" pressure increment $\Delta p_{\text{inv.}}/p_\infty$ from the measurement pressure on the flat surface; the results are shown in Fig. 12. In spite of the scatter of the data, it is clear that the inviscid rotational flow effects associated with the strong detached bow wave account for a large part of the observed behavior.‡

For weak or moderate shock waves, Friedrichs[59] and Lighthill[60] have shown quite generally that the leading-edge shock strength, as measured by flow deflection, varies as the inverse square root of the distance along the shock from the leading edge when this distance is large compared with the airfoil chord. Lighthill utilizes this result, and others derived by him, to explain the behavior of blunt-nosed slender airfoils at transonic and moderate supersonic speeds. An approximate solution of Eq. (4-3) in Lighthill's article[60] shows that $\theta_2 \sim (1/x^{1/5})$ for strong shocks in air, †† so that, on this basis, the strength of the reflected pressure waves $\Delta p_R/p_\infty$ in our problem would be expected to vary as $M_\infty{}^2/(x/t)^{2/5}$ near the leading edge. Further downstream, Lighthill's work shows that $(\Delta p_R/p_\infty) \cong M_\infty{}^3/(x/t)^{3/2}$. This rather slow decay of the leading-edge shock means that a considerable drag is associated with the leading edge at hypersonic speeds. [See Fig. E, 5d, reference 60 for $M_\infty = 0(1)$.] A portion of this drag occurs as pressure drag on the nose itself, while the rest appears as increased skin-friction drag on the surface parallel to the flight direction because of the strong favorable pressure gradients extending many leading-edge thicknesses downstream. Much work remains to be done on this interesting problem.

(4) Hypersonic Flow over Blunt Bodies

(4.1) Inviscid Flow

When the considerable body of experimental data on pressure distributions over hemisphere cylinders is re-examined, the Newtonian $\sin^2\theta_b$ law is confirmed for $M_\infty > 2$ (approximately). Usually the data are compared with the simple expression $C_p = 2\sin^2\theta_b = 2\cos^2\theta$, where θ is the ray angle from the stagnation point. But for a real gas the pressure rise across the normal shock is given by

$$p_2 - p_\infty = \rho_\infty U_\infty{}^2[1 - (\rho_\infty/\rho_2)]$$

and the pressure recovery between the shock wave and the stagnation point is

$$p_0{}^1 - p_2 \cong (1/2)\rho_2 u_2{}^2 = (1/2)\rho_\infty U_\infty{}^2(\rho_\infty/\rho_2)$$

Therefore, $p_0{}^1 - p_\infty \cong p_\infty U_\infty{}^2[1 - (1/2)(\rho_\infty/\rho_2)]$

† This behavior contrasts with the situation at transonic speeds, where the reflected waves are compressions.

‡ A more realistic "model" would be a blunt leading edge followed by a parabolic body.

†† Actually $\theta \sim \frac{1}{x^k}$ where $k = \dfrac{\sqrt{(\gamma-1)/2}\,[\sqrt{\gamma} - \sqrt{(\gamma-1)/2}]}{1 + \sqrt{[\gamma(\gamma-1)]/2}}$

and $C_{p_{max}} \cong 2 - (\rho_\infty/\rho_2) = (\gamma + 3)/(\gamma + 1)\,[1 - (2/\gamma + 3)(1/M_\infty^2)] < 2$. This result suggests that it would be more revealing to compare the ratio $C_p/C_{p_{max}}$ with $\cos^2\theta$, and such a comparison is shown in Fig. 13 for the Mach Number range $1.97 < M < 5.8$ over a Reynolds Number range of $2.4 \times 10^5 < Re_D < 2.8 \times 10^6$. For $M_\infty \cong 2$ the over-expansion on the shoulder is quite noticeable, but at $M_\infty = 5.8$ the pressure is already considerably larger than free stream. It is interesting that the pressure on the shoulder is very close to free stream at a Mach Number (≈ 3.3) such that the calculated drop in pressure from stagnation to sonic point ($\theta_b \cong 45°$), followed by a Prandtl-Meyer expansion to $\theta_b = 0$, is in fact just about equal to the pressure rise from free stream to stagnation point. The over-pressure on the shoulder for $M_\infty > 3.3$ is closely connected with the blunt leading-edge effect already discussed in Section (3.3).

A test of the purely local dependence of pressure on surface inclination is provided by a body with a rapidly changing or even discontinuous radius of curvature, such as a 40° half-angle cone with a spherical cap. The pressure distribution over such a body at $M_\infty = 5.8$ (Fig. 14) shows a slight over-expansion beyond the sonic point and a rapid recovery to the theoretical value predicted for a semi-infinite cone. Some evidence of viscous effects is apparent at the lower Reynolds Numbers.

A quantity of considerable importance in the heat-transfer problem for blunt bodies is the velocity gradient along the outer edge of the boundary layer [Section (4.2)]. Now

$$u_\delta^2/u_\infty^2 = \{1 + [2/(\gamma - 1)](1/M_\infty^2)\}\,[1 - (p_\delta/p_0{}^1)^{\frac{\gamma - 1}{\gamma}}]$$

But
$$p_\delta/p_0{}^1 \cong 1 - \sin^2\theta$$

so that
$$u_\delta/u_\infty \cong \sqrt{(\gamma - 1)/\gamma}\,\sqrt{1 + [2/(\gamma - 1)](1/M_\infty^2)}\,\sin\theta \times [1 + (1/4\gamma)\sin^2\theta + \ldots]$$

The velocity is very nearly linear in θ up to $\theta \cong \pi/2$, as compared with the $\sin\theta$ variation at low speeds for a sphere. The initial gradient at the stagnation point is given by

$$\tilde{u}_0{}^1 = \left(\frac{D}{u_2}\frac{du_\delta}{ds}\right)_{s=0} = 2\,\frac{\gamma + 1}{\sqrt{\gamma(\gamma - 1)}}\,\frac{1}{\sqrt{1 + [2/(\gamma - 1)](1/M_\infty^2)}} \quad \text{for } M_\infty > 4 \text{ (approx.)}$$

where u_2 is the axial velocity just behind the shock wave.

In the limit $M_\infty \to \infty$ the initial velocity gradient approaches a value of 6.4 for a diatomic gas and 9.0 for $\gamma = 1.20$, compared with 3.0 for the low-speed flow over a sphere and 4.0 for a cylinder. Thus at high Mach Numbers $\tilde{u}_0{}^1$ is quite sensitive to the thermodynamic processes occurring in the gas near the stagnation point.

(4.2) Heat Transfer over Blunt Bodies

At ultra-high-flight speeds all bodies are blunt-nosed to some extent, and the maximum heat-transfer rates on the body may occur near the forward stagnation point. Since the flow is subsonic there, Sibulkin[61] suggested that a "low-speed"

solution, using quantities evaluated just behind the shock as free-stream conditions, might be a good first approximation. When viscous dissipation and the pressure work term are neglected and the fluid properties are regarded as constant, the boundary-layer momentum equation near the forward stagnation point of a body of revolution is identical with Homann's[62] low-speed equation, which in turn is a special case of the Falkner-Skan[47] equation with $\beta = (1/2)$. The energy equation is readily integrated numerically, using Homann's velocity distribution, and Sibulkin found that the local heat-transfer rate at the forward stagnation point is given by

$$Nu_D = (hD/k_2) = 0.763(Pr)^{0.4} \sqrt{\tilde{u}_0^1} \sqrt{u_2 D/\nu_2}$$

where $\tilde{u}_0^1 = [(D/u_2)(du_\delta/ds)]_0$. Here h is defined by $q = h(T_s - T_w)$. For a blunt-nosed cylinder[63] the value of the constant is 0.570. Sibulkin utilized the low-speed value of 3.0 for $\tilde{u}_0^1$. Later,† he extended his analysis to the rest of the hemisphere by assuming that the velocity and temperature profiles are similar and of a parabolic shape, and he employed the momentum and energy integral methods to evaluate the constants. The result is

$$Nu_D = K(\theta)(Pr)^{0.4} \sqrt{u_2 D/\nu_2}$$

where $K(\theta)$ is a rather slowly varying function of the ray angle θ measured from the stagnation point. The value of $K(0)$ is about 10 per cent higher than Sibulkin's original value at the stagnation point. Korobkin[64] later showed that the choice of profiles is not critical; all of his approximate solutions have about the same variation with angle and differ by no more than 15 per cent from the original value at $\theta = 0$.

A similar approach to the heat-transfer problem over a hemispherical nose at supersonic speeds is contained in a recent report by Stine and Wanlass.[65] Like Korobkin and Sibulkin, they restrict their analysis to the case where the difference between stagnation temperature and surface temperature is small compared with the stagnation temperature. Instead of using integral methods, they combine Mangler's transformation and the Stewartson-Illingworth transformation to reduce the momentum equation to the Falkner-Skan equation, where the pressure gradient parameter β is now a function of angular position. The main simplifying assumption is similar to Sibulkin's,[64] namely that at every point on the body the "reduced" velocity and temperature profiles are identical with those obtained from the Falkner-Skan "similar" solutions corresponding to the local value of β. With the aid of this assumption, the distribution of heat-transfer rate over an isothermal blunt-nosed body of revolution can be calculated entirely from the theoretical or experimental pressure distribution.

Just as in the theoretical work, experimental investigations of this problem have so far been restricted to the case of small temperature differences. The main experimental difficulties are: (1), heat conduction within the body shell which introduces errors into the local heat balance equation; and (2), nonuniform surface temperature, which is known to have an important influence on local heat-transfer rates. Korobkin's[66] measurements in the NOL blow-down tunnel at $M = 2.8$ were slightly lower than the theoretical values, even after the $K(\theta)$ curve is "ad-

† Unpublished, but reported by Korobkin.[64]

justed'' so that it passes through Sibulkin's original stagnation-point-value. A rough correction for axial temperature gradients brings the two curves closer together: their shape is very similar. At $M_\infty = 2.8$ the measured value of $\tilde{u}_0'$ is about 4.5, as compared with 3.0 in the Sibulkin theory, so the discrepancy may be even larger than it appears. Later NOL results[67] show much closer agreement with the Sibulkin-Korobkin analysis in the range $1.90 < M_\infty < 4.87$, provided that the *actual measured value* of $\tilde{u}_0'$ is used in the calculation of Nu_D. Similar remarks apply to the measurements of Stine and Wanlass.[65] In fact, these authors state (p. 18) that the theoretically predicted distribution is probably better than the experiments because the experimental scatter is about ± 18 per cent, while uncertainties in the calculation are about ± 15 per cent. It is interesting that the values of $Nu_x/\sqrt{Re_x}$ on the hemisphere-cylinder drop below the theoretical cone-cylinder values near the shoulder and approach the flat plate value of $0.332\ Pr^{1/3}$ more rapidly than for the cone-cylinder.

Stine and Wanlass do not mention the fact that their method can be generalized to the case of large temperature differences. If the transformation employed by Levy[43] is modified somewhat and combined with the Mangler transformation, the Nusselt Number (at the stagnation point *based on physical properties evaluated at the surface temperature*) has the same form as Sibulkin's original expression. Suppose that

$$\tilde{s} = \int_0^x \mu_w \rho_w u_\delta r_0^2 ds \quad \text{and} \quad \eta = \frac{\rho_\delta u_\delta}{(2s)^{1/2}} \int_0^y r_0 \frac{\rho}{\rho_\delta}\, dy$$

where $r_0(x)$ is the radius of the body cross section normal to the x-axis. Then the boundary-layer momentum equation for a body of revolution is again reduced to the Falkner-Skan equation, with

$$\beta = (2\tilde{s}/M_\delta)(dM_\delta/d\tilde{s})$$

At the stagnation point, for example, $r_0 \cong x$, and the energy equation reduces to the same form as the low-speed heat-transfer equation for arbitrary Prandtl Number. Also $\beta = (1/2)$. We write down immediately that

$$\frac{hD}{k_w} = \sqrt{\left(\frac{D}{u_2}\frac{du_\delta}{ds}\right)_0}\sqrt{\frac{\rho_w u_2 D}{\mu_w}}\left\{\frac{\sqrt{2}\, g'[0; Pr; (T_w/T_{s_\infty})]}{\kappa}\right\}_{\beta=1/2}$$

where

$$\kappa = 1 - (T_w/T_{s_\infty})$$

and the prime means differentiation with respect to η. The function

$$\left\{\frac{g'[0; Pr; (T_w/T_\infty)]}{\kappa}\right\}_{\beta=1/2}$$

is given in Fig. 10 of Levy's paper for $Pr = 0.7$ and 1.0, for values of $T_w/T_{s_\infty} = g(0)$ of 0.60, 0.80, 1.0, 1.5, and 2.0. For $Pr = 1$ a much wider range of values of T_w/T_{s_∞} is covered in the work of Cohen and Reshokto.[44] Here $[g'(0)/\kappa] = (s_w'/s_w)$. There does not seem to be any difficulty in extending the Stine and Wanlass procedure to the rest of the hemisphere. For a blunt-nosed cylinder, $\beta = 1$ and the factor $\sqrt{2}$ in the brackets disappears.

At hypersonic flight speeds, the gas can no longer be regarded as an ideal gas with a certain average ratio of specific heats across the boundary layer. However, the relation between density and enthalpy enters the problem explicitly only in the pressure gradient term in the momentum equation. If $T_w/T_{s_\infty} \ll 1$, as in many aeronautical applications, the pressure gradient term has only a small effect, as remarked in Section (3.2) (see also Fig. 9, reference 44, for $S_w = -1, -0.8$). In this case, the value of $[g'(0)/\kappa] \rightarrow g'(0)$ should not differ appreciably from the "Blasius value" of $0.47Pr^{1/3}$.

All of these considerations are based on the assumption of thermodynamic equilibrium and conventional fluid mechanics. This well-defined problem of heat transfer on a blunt body would seem to be a fruitful one for the exploration of the possible influence of nonequilibrium processes at high stagnation temperature.

References

[1] Tsien, H. S., *Similarity Laws of Hypersonic Flows*, J. of Math. and Physics, Vol. 25, No. 3, pp. 247–251, October, 1946.

[2] Hayes, W., *On Hypersonic Similitude*, Quart. of Applied Math., Vol. V, No. 1, pp. 105–106, April, 1947.

[3] Ehret, D. M., Rossow, V. J., and Stevens, V. I., *An Analysis of the Applicability of the Hypersonic Similarity Law to the Study of the Flow about Bodies of Revolution at Zero Angle of Attack*, NACA TN 2250, 1950.

[4] Niece, S. E., and Ehret, D. M., *Similarity Laws for Slender Bodies of Revolution in Hypersonic Flows*, Journal of the Aeronautical Sciences, Vol. 18, No. 8, pp. 527–530, p. 568, August, 1951.

[5] Rossow, V. J., *Applicability of the Hypersonic Similarity Rule to Pressure Distributions Which Include the Effects of Rotation for Bodies of Revolution at Zero Angle of Attack*, NACA TN 2399, 1951.

[6] Hamaker, F. M., Neice, S. E., and Eggers, A. J., Jr., *The Similarity Law for Hypersonic Flow About Slender Three-Dimensional Shapes*, NACA TN 2443, 1951.

[7] Hamaker, F. M., and Wong, T. J., *The Similarity Law for Nonsteady Hypersonic Flows and Requirements for the Dynamic Similarity of Related Bodies in Free Flight*, NACA TN 2631, 1952.

[8] Van Dyke, M. D., *The Combined Supersonic-Hypersonic Similarity Rule*, Journal of the Aeronautical Science, Vol. 18, No. 7, pp. 499–500, July, 1951.

[9] von Kármán, Th., *The Problem of Resistance in Compressible Fluids*, Proc. of the 5th Volta Congress, Rome, 1935, pp. 210–271, esp. pp. 269–271 (GALCIT Publication No. 75, 1936).

[10] Busemann, A., *Flussigkeits-und Gasbewegung*, Handwörterbuch der Naturwissenschaften, pp. 275–277, Zweite Auflage (Gustav Fischer, Jena), 1933.

[11] Grimminger, G., Williams, E. P., and Young, G. B. W., *Lift on Inclined Bodies of Revolution in Hypersonic Flow*, Journal of the Aeronautical Sciences, Vol. 17, No. 11, p. 675–690, November, 1950.

[12] Ivey, H. R., Klunker, E. G., and Bowen, E. N., *A Method for Determining the Aeronynamic Characteristics of Two- and Three-Dimensional Shapes at Hypersonic Speeds*, NACA TN 1613, 1948.

[13] Epstein, P. S., *On the Air Resistance of Projectiles*, Proc. National Acad. of Sci., Vol. 17, No. 9 pp. 532–547, September, 1931.

[14] Eggers, A. J., Jr., and Savin, R. C., *Approximate Methods for Calculating the Flow about Non-Lifting Bodies of Revolution at High Supersonic Airspeeds*, NACA TN 2579, 1951.

[15] Eggers, A. J., Jr., and Syvertson, C. A., *Inviscid Flow About Airfoils at High Supersonic Speeds*, NACA TN 2646, 1952.

[16] Eggers, A. J., Jr., *On the Calculation of Flow About Objects Travelling at High Supersonic Speeds*, NACA TN 2811, 1952.

[17] Eggers, A. J., Jr., and Kraus, S., *Approximate Calculation of Axisymmetric Flow Over the Vertex of a Body Travelling at High Supersonic Speeds*, Journal of the Aeronautical Sciences, Vol. 20, No. 3, pp. 215–217, March, 1953.

[18] Eggers, A. J., Jr., Savin, R. C., and Syvertson, C. A., *The Generalized Shock-Expansion Method and its Application to Bodies Travelling at High Supersonic Airspeeds*, paper presented at Annual Summer Meeting, I.A.S., Los Angeles, Calif., June 21–24, 1954. Preprint No. 478.

[19] Shen, S. F., *An Estimate of Viscosity Effect on the Hypersonic Flow Over an Insulated Wedge*, J. Math. and Physics, Vol. 31, No. 3, pp. 192–205, October, 1952 (Based on Part I of a Sc.D. Thesis, Dept. of Aero. Eng., M.I.T., 1949).

[20] Döring, W., and Burkhardt, H., *Beiträge zur Theorie der Detonation*, Chapter II, Brown University Translation, TR F-TS-1227-IA (GDAM, A9-T-46), 1949.

[21] Bethe, H. A., and Teller, E., *Deviations from Thermal Equilibrium in Shock Waves*, Report No. X-117, Ballistic Res. Lab., Aberdeen Proving Ground, 1945.

[22] Resler, E. L., Lin, S. C., and Kantrowitz, A., *The Production of High Temperature Gases in Shock Tubes*, J. Applied Physics, Vol. 23, No. 12, pp. 1,390–1,399, December, 1952. Also Kantrowitz, A., *Strong Shock Waves*, paper presented at Conference on High Speed Aeronautics sponsored by Polytechnic Inst. of Brooklyn, New York, January 22, 1955.

[23] Ivey, H. R., and Cline, C. W., *Effect of Heat-Capacity Lag on the Flow Through Oblique Shock Waves*, NACA TN 2196, 1950.

[24] Kraus, S., *An Analysis of Supersonic Flow in the Region of the Leading-Edge of Curved Airfoils, Including Charts for Determining Surface-Pressure Gradient and Shock-Wave Curvature*, NACA TN 2729, 1952.

[25] Kahane, A., and Lees, L., *The Flow at the Rear of a Two-Dimensional Supersonic Airfoil*, Journal of the Aeronautical Sciences, Vol. 15, No. 3, pp. 167–170, March, 1948.

[26] Linnell, R. D., *Two-Dimensional Airfoils in Hypersonic Flow*, Journal of the Aeronautical Sciences, Vol. 16, No. 1, pp. 22–30, January, 1949.

[27] von Kármán, Th., "On the Foundation of High Speed Aerodynamics," Section A, Volume VI, *General Theory of High Speed Aerodynamics*, pp. 3–30, Series on High Speed Aerodynamics and Jet Propulsion; Princeton Univ. Press, 1954.

[28] Van Dyke, M. D., *Applications of Hypersonic Small-Disturbance Theory*, Journal of the Aeronautical Sciences, Vol. 21, No. 3, pp. 179–186, March, 1954.

[29] Van Dyke, M. D., *A Study of Hypersonic Small-Disturbance Theory*, NACA TN 3173, 1954.

[30] Halbmillion, V., and Kulishek, C. J., *Geometric and Aerodynamic Data on Ogives*, NAVORD Rept. 2239, January 17, 1952, U. S. Naval Ordnance Laboratory, White Oak, Md.

[31] Lees, L., *Note on the Hypersonic Similarity Law for an Unyawed Cone*, Journal of the Aeronautical Sciences, Vol. 18, No. 10, pp. 700–702, October, 1951.

[32] Staff of the Computing Section, Center of Analysis, M.I.T., under the direction of Zdenek Kopal, *Tables of Supersonic Flow Around Cones*, Technical Report No. 1, 1947.

[33] Cabannes, H., *Etude de L'Onde de Choc Attachée dans les Écoulements de Revolution*, Premiere Partie: Cas d'un Obstacle Terminé par une Ogive, La Recherche Aéronautique, No. 24, pp. 17–23, Novembre-Decembre, 1951.

[34] Probstein, R. F., and Bray, K. N. C., *Hypersonic Similarity and the Tangent-Cone Approximation for Unyawed Bodies of Revolution*, Journal of the Aeronautical Sciences, Vol. 22, No. 1, pp. 66–68, January, 1955.

[35] Ferri, A., *Supersonic Flow Around Circular Cones at Angles of Attack*, NACA TN 2236, 1950.

[36] Lees, L., *On the Boundary Layer Equations in Hypersonic Flow and Their Approximate Solutions*, Journal of the Aeronautical Sciences, pp. 143–145, Vol. 20, No. 2, February, 1953.

[37] Lees, L., and Probstein, R. F., *Hypersonic Viscous Flow Over a Flat Plate*, Princeton University, Aeron. Engrg. Lab. Report No. 195, April 20, 1952.

[38] Lees, L. and Probstein, R. F., *Monograph on Hypersonic Flows of a Viscous Fluid* (in preparation).

[39] Stewartson, K., *On the Motion of a Flat Plate at High Speeds in a Viscous Compressible Fluid—Part II. Steady Motion*, Journal of the Aeronautical Sciences, Vol. 22, No. 5, pp. 303–309, May, 1955.

[40] Nagamatsu, H. T., and Li, Ting-Yi, *Shock Wave Effects on the Laminar Skin Friction of an Insulated Flat Plate at Hypersonic Speeds*, Journal of the Aeronautical Sciences, Vol. 20, No. 5, pp. 345–355, May, 1953.

[41] Lees, L., *Influence of the Leading-Edge Shock Wave on the Laminar Boundary Layer at Hypersonic Speeds*, GALCIT, Technical Report No. 1, July 15, 1954.

[42] Lees, L., *Hypersonic Viscous Flow over an Inclined Wedge*, Journal of the Aeronautical Sciences, Vol. 20, No. 11, pp. 794–795, November, 1953.

[43] Levy, S., *Effect of Large Temperature Changes (Including Viscous Heating) upon Laminar Boundary Layers with Variable Free-Stream Velocity*, Journal of the Aeronautical Sciences, Vol. 21, No. 7, pp. 459–474, July, 1954.

[44] Cohen, C. B., and Reshotko, E., *Similar Solutions for the Compressible Laminar Boundary Layer with Heat Transfer and Pressure Gradient*, NACA TN 3325, 1955.

[45] Li, Ting-Yi, and Nagamatsu, H. T., *Similar Solutions of Compressible Boundary-Layer Equations*, Journal of the Aeronautical Sciences, Vol. 20, No. 9, pp. 653–655, September, 1953. Also Proc. 1954 Heat Transfer and Fluid Mech. Institute, p. 143.

[46] Li, Ting-Yi, and Nagamatsu, H. T., *The Effect of Heat Transfer on the Behavior of a Compressible Laminar Boundary Layer Under Favorable and Adverse Pressure Gradients*, Journal of the Aeronautical Sciences, Vol. 21, No. 12, pp. 850–851, December, 1954.

[47] Falkner, V. M., and Skan, S. F., *Some Approximate Solutions of the Boundary Layer Equations*, British A.R.C., R and M. No. 1314, 1930.

[48] Hartree, D. R., *On An Equation Occurring in Falkner and Skan's Approximate Treatment of the Equation of the Boundary Layer*, Proc. Cambridge Phil. Soc., Vol. 33, Pt. 2, pp. 233–239, April, 1937.

[49] Crocco, L., *Lo Strato Limite Laminare nei Gas*, Monografie Scientifiche di Aeronautica No. 3, Associazone Culturale Aeronautica, Roma, 1946. Translated as Aerophysics Lab. Report AL-684, North American Aviation, Inc., Downey, Calif., 1948.

[50] Becker, J. V., *Results of Recent Hypersonic and Unsteady Flow Research at the Langley Aeronautical Laboratory*, J. Appl. Physics, Vol. 21, No. 7, pp. 619–628, July, 1950.

[51] Maslen, S. H., *Second Approximation to Laminar Compressible Boundary Layer on a Flat Plate in Slip-Flow*, NACA TN 2818, 1952.

[52] Bertram, M. H., *An Approximate Method for Determining the Displacement Effects and Viscous Drag of Laminar Boundary Layers in Two-Dimensional Hypersonic Flow*, NACA TN 2773, 1953.

[53] Probstein, R. F., and Elliott, D., *Hypersonic Viscous Flow Over a Cone*, Princeton University, Aero. Engrg. Dept., 1953 (unpublished).

[54] Lin, T. C., Schaaf, S. A., and Sherman, F. S., *Boundary Layer Effect on the Surface Pressure of an Infinite Cone in Supersonic Flow*, Univ. of California Rep. No. HE-150-80, NACA Contract NAw-6004, March 5, 1951.

[55] Talbot, L., *Viscosity Corrections to Cone Probes in Rarefied Supersonic Flow at a Nominal Mach Number of 4*, NACA TN 3219, 1954.

[56] Probstein, R. F., and Elliott, D., *The Transverse Curvature Effect in Compressible Axially-Symmetric Boundary Layer Flow*, Princeton University, Dept. Aeron. Engrg., Report No. 261, 1954 (To be published in the Journal of the Aeronautical Sciences).

[56a] Kuo, Y. H., *Viscous Flow Along a Flat Plate Moving at High Supersonic Speeds*, Cornell University, Graduate School of Aeronautical Engineering, 1954.

[57] Bertram, M. H., *Viscous and Leading-Edge Thickness Effects on the Pressures on the Surface of a Flat Plate in Hypersonic Flow*, Journal of the Aeronautical Sciences, Vol. 21, No. 6, pp. 430–431, June, 1954.

[58] Hammitt, A. G., and Bogdonoff, S. M., *A Study of the Flow About Simple Bodies at Mach Numbers from 11 to 15*, WADC Technical Report 54-257, October, 1954.

[59] Friedrichs, K. O., *Formation and Decay of Shock Waves*, Comm. Pure and Appl. Math., Vol. 1, p. 211, 1948.

[60] Lighthill, M. J., "Higher Approximations," Section E, esp. E. 4, pp. 396–406, and E. 5., Vol. VI, *General Theory of High Speed Aerodynamics*, Series on High Speed Aerodynamics and Jet Propulsion; Princeton University Press, Princeton, N. J., 1954.

[61] Sibulkin, M., *Heat Transfer Near the Forward Stagnation Point of a Body of Revolution*. Journal of the Aeronautical Sciences, Vol. 19, No. 8, pp. 570–571, August, 1952.

[62] Goldstein, S., *Modern Developments in Fluid Dynamics*, Vol. 1, p. 142; Oxford University Press, London, 1938.

[63] Goldstein, S., *Modern Developments in Fluid Dynamics*, Vol. 2, pp. 631–632.

[64] Korobkin, I., *Discussion of Laminar Heat Transfer Coefficients for Spheres and Cylinders in Compressible Flow*, Paper presented at ASME Fall Meeting, Milwaukee, Wisconsin, September 9, 1954.

[65] Stine, H. A., and Wanlass, K., *Theoretical and Experimental Investigation of Aerodynamic-Heating and Isothermal Heat-Transfer Parameters on a Hemispherical Nose with Laminar Boundary Layer at Supersonic Mach Numbers*, NACA TN 3344, 1954.

[66] Korobkin, I., *Local Flow Conditions, Recovery Factors and Heat Transfer Coefficients on the Nose of a Hemisphere Cylinder at a Mach Number of 2.80*, NAVORD Rept. 2865, May 5, 1953, U. S. Naval Ordnance Laboratory, White Oak, Md.

[67] Gruenewald, K. W., and Lobb, R. K., *New Laminar and Turbulent Heat Transfer Data Applicable to Practical Body Shapes for High Mach Number Flight*, paper presented at U. S. Navy Symposium on Aeroballistics, sponsored by BuOrd at the Applied Physics Laboratory, Silver Spring, Md., October 19 and 20, 1954.

Appendix

Estimate of Errors in the Tangent-Wedge Approximation in the Limiting Case $K_b \to \infty$

As discussed in Section (2.1), the tangent-wedge approximation neglects centrifugal force and also contains the assumption that the velocity component normal to the flight direction (or the flow inclination) is unchanged along a normal from body surface to shock. In order to estimate these errors in the limiting case $K_b \to \infty$, it is convenient to write the continuity and momentum equations in local, plane polar coordinates (Fig. 4). In this system, the continuity equation is

$$(u_r/\rho)(\partial\rho/\partial r) + (u_\theta/\rho r)(\partial\rho/\partial\theta) + (\partial u_r/\partial r) + (u_r/r) + (1/r)(\partial u_\theta/\partial\theta) = 0$$

while the momentum equation in the direction normal to the radius is

$$\rho[u_r(\partial u_\theta/\partial r) + (u_\theta/r)(\partial u_\theta/\partial\theta) + (u_\theta u_r/r)] = -(1/r)(\partial p/\partial\theta)$$

But $u_\theta = 0$ on the body and $u_\theta/u_\infty \cong -(\theta_s - \theta_b)$ at the shock and is small compared with θ_b; therefore, in this calculation terms of order $[(\theta_s - \theta_b)/\theta_b]^2$ are neglected. Also, $u_r \cong u_\infty$, to this order.

Since the body is slender and the body surface is a streamline

$$(u_r/\rho)(\partial\rho/\partial r) \cong (1/\gamma)(u_\infty/p)(\partial p/\partial s) = (2u_\infty/\gamma)(\kappa/\theta_b) \qquad \text{for } K_b \gg 1,$$

where s is distance along the body surface and $\kappa = (d\theta_b/ds)$ is the curvature. From the continuity equation

$$\partial u_\theta/\partial_\theta \cong -u_\infty[1 + (2/\gamma)(\kappa/\theta_b)r] + 0[(\theta_s - \theta_b)/\theta_b]$$

Therefore, u_θ at the shock is given approximately by

$$-u_\infty[1 + (2/\gamma)(\kappa/\theta_b{}^2)z_b](\theta_s - \theta_b)$$

since $r \cong (z/\theta_b)$. But the shock condition is

$$(u_\theta/-u_\infty\theta_s) = (\rho_\infty/\rho_2) = (\gamma - 1)/(\gamma + 1)$$

so that

$$\theta_s \cong [(\gamma + 1)/2]\theta_b\{1 - [(\gamma - 1)/\gamma]z_b(\kappa/\theta_b{}^2)\}$$

and the pressure just behind the shock wave is

$$p_2/p_\infty \cong \{[\gamma(\gamma + 1)]/2\} M_\infty{}^2\theta_b{}^2 - (\gamma^2 - 1) M_\infty{}^2 z_b \kappa$$

The only term in the momentum equation that does not contribute terms of order $[(\theta_s - \theta_b)/\theta_b]^2$ to the pressure difference $p_2 - p_b$ is the centrifugal force—i.e., $p_2 - p_b \cong -(\rho u^2 \kappa)(z_s - z_b)$. But by continuity $\rho u(z_s - z_b) \cong \rho_\infty u_\infty z_b$, so that $p_2 - p_b \cong \rho_\infty u_\infty{}^2 z_b \kappa$†

Finally,

$$(p_b/p_\infty) \cong \{[\gamma(\gamma + 1)]/2\} M_\infty{}^2\theta_b{}^2 + M_\infty{}^2 z_b \kappa[\gamma - (\gamma^2 - 1)]$$

DISCUSSION‡

S. M. Bogdonoff: I would like to compliment Professor Lees on his excellent presentation and to add a few comments based on our work in this hypersonic range. The field is, as he put it, wide open at the moment, and I would like to take exception to a few things that Professor Lees mentioned in his paper. At Princeton's Gas Dynamics Laboratory, we have carried out many tests at Mach Numbers from 11 to 14 on sharp, flat plates. We have found that there appears to be an inconsistency in the general framework in which we treat the boundary layer and the inviscid flows. If we take a set of experimental data on boundary-layer profiles and shock shapes from a flat plate with a sharp leading edge, it is found that the region outside of the boundary layer (between the edge of the boundary layer and the shock) can be predicted by knowing the shock shape and the pressure distribution on the plate using the inviscid method of characteristics including variable entropy. However, the techniques usually used to predict the thickness of the boundary layer appear to be off by a factor of at least 2. That is, the actual boundary layer appears to be about twice as thick as any that can be calculated. We always come back to the question of what happens exactly at the leading edge. Our more recent work has shown that the entire flow is almost completely determined by the leading edge even though it may be of dimensions quite small as compared to any other dimensions involved.

With regard to blunt bodies, one word of caution. The idea of being able to simulate the flow around the blunt body by the test at a lower Mach Number is inaccurate. You can, perhaps, get the right pressures and temperatures at the stagnation point and in some regions around the stagnation point, but you cannot simulate the strong entropy field that occurs because of the strong shocks and high curvatures. Tests that we have carried out have shown that this effect is not negligible if there is any interest in the region beyond the stagnation point. Although the idea of simulating the flow may be a good first approximation, it may be far from the real answer over a large part of the body after the nose.

Jackson Stalder: We have recently obtained data that corroborates Professor

† See also references 10–12 for the calculation of centrifugal force on a body.

‡ Names and affiliations of all Discussers may be found on pp. 559–560.

Lees argument about blunt bodies. We have measured heat-transfer rates on a hemispherical nose of a cylinder and found that, by evaluating the air properties and conditions behind the normal shock wave, we were able to correlate all the heat-transfer data obtained over a Mach Number range of from two-tenths to five. I do not know how this fits into Professor Bogdonoff's statement just made. Perhaps he can enlighten us. These data were semilocal. The heat transfer was measured on the forward half area and the rearward half area of the hemisphere.

S. M. Bogdonoff: The approximation is very good at stagnation point. You can simulate flows at stagnation points. These results do check very well. Once we deviate from the stagnation point, we have found large differences. Of course yours is a much larger scale, integrated over much larger areas than ours.

J. Stalder: Of course, also, the heat transfer at stagnation point is so high, as compared to the remainder of the cylinder, it is the effect that predominates.

I. I. Glass: I wonder if Professor Bogdonoff or some people in NACA would like to comment. Essentially, perhaps you can simulate flow. If you have a blunt body in a shock tube up to the sonic line, when you do get expansion around the corner, the importance of high Mach Number would show up in the afterbody.

S. M. Bogdonoff: I am sorry; I seem to have ended up in the middle of this. We ought to get back to Professor Lees and his questions. For myself, it was just a word of warning that we can simulate things close to the stagnation point or some distance from the stagnation point. But let's not delude ourselves that we can go very much beyond. It is a question that must be answered. I simply brought up the point that there are strong gradients because of strong curvature. If you have strong shocks in the frame, these entropic gradients cannot be—this is where it becomes important. Perhaps the sonic point is a good point to bring it from here on. I think it is a point of getting essentially the measurements.

L. Lees: I would like to make a more precise statement about the modified Newtonian approximation. Whenever the product of Mach Number and sine of the body inclination angle is large compared with one, what I said is correct. The amazing thing to me is the fact that the idea holds in practice to much lower values of $M_\infty \sin \theta_b$ than anyone would have expected. Thus the pressure distribution and velocity gradient along the body, which are essential in heat-transfer work, can be taken from the modified Newtonian theory, at least up to $\theta = 60°$. Of course this theory includes the effect of the vorticity and the strong entropy gradient.

When you come around the body to the region where $M_\infty \sin \theta_b < 1$ then Professor Bogdonoff is right, and the flow is influenced very strongly by the conditions near the nose, as illustrated by a recent calculation we made on the boundary-layer development over a hemispherical nose followed by a cylindrical afterbody. But there does not seem to be any inconsistency in the separation of the flow into inviscid and viscous flow regions.